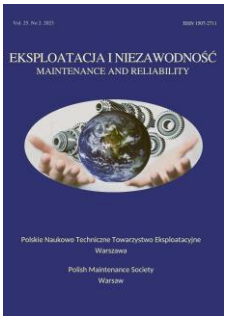

Eksploatacja i Niezawodnosc – Maintenance and Reliability
Volume 28 (2026), Issue 4
journal homepage: http://www.ein.org.pl

Article citation info:
Zhao C, Xiang S, Niu F, Li K, Predicting remaining useful life of AC contactors based on a novel doubly truncated degradation model considering arcing mode transitions, Eksploatacja i Niezawodnosc – Maintenance and Reliability 2026: 28(4) http://doi.org/10.17531/ein/220210

Predicting remaining useful life of AC contactors based on a novel doubly truncated degradation model considering arcing mode transitions

Indexed by: Web of Science Group

Changdong Zhao[a,b], Shihu Xiang[a,b,*], Feng Niu[a,b], Kui Li[a,b]

[a] State Key Laboratory of Smart Power Distribution Equipment and System, Hebei University of Technology, Tianjin, China
[b] Key Laboratory of Electromagnetic Field and Electrical Apparatus Reliability of Hebei Province, Hebei University of Technology, Tianjin, China

Highlights

- Bounds of arcing Joule integral are derived by introducing critical phase angles.
- Four arcing modes are identified based on the presence or absence of arcing.
- Novel doubly truncated degradation model considering arcing mode transition is given.
- Real and numerical cases are used to verify the efficacy of the proposed method.

Abstract

Accurate remaining useful life (RUL) prediction of AC contactors is essential for efficient operation and maintenance of the manufacturing system. Existing methods cannot adequately capture the degradation of AC contactors due to their inability to depict the special characteristic of zero and bounded arcing Joule integrals (i.e., degradation increments). To tackle this problem, the physical model of arcing Joule integrals is first derived through arcing mechanism analysis. Bounds of arcing Joule integrals are obtained by introducing critical breaking phase angles to the physical model, and four arcing modes are identified. A method for measuring the similarity between arcing modes is proposed, and then an arcing mode similarity based discrete-time Markov chain is constructed to depict arcing mode transitions. Motivated by zero and bounded arcing Joule integrals, an increment process with zero and bounded increments is proposed to characterize the degradation of a single-phase contact pair. Finally, the superiority of the proposed method is illustrated by real and numerical cases.

Keywords
AC contactor, multiple arcing modes, nonlinear degradation correlation, remaining useful life prediction, zero and bounded degradation increments

1. Introduction

AC contactors are widely utilized in manufacturing systems, where they play a crucial role in controlling a system to perform its intended functions or in protecting a system from accidents [1,2]. The failure of an AC contactor can endanger the system, potentially resulting in severe consequences such as production disruptions, casualties, and environmental damages [3,4]. Therefore, accurately predicting the remaining useful life (RUL) of AC contactors is imperative. This enables appropriate operation and maintenance decision-making, as well as efficient production planning, ensuring safe and stable operation of the system and contributing to both product quality and manufacturing efficiency [5,6].

The intricate failure mechanism of AC contactors leads to complex degradation processes, which exhibit characteristics such as competing failure and multiple arcing modes. The characteristic of competing failure can be analyzed as follows. An AC contactor has three pairs of contacts, corresponding to phases A, B, and C. The failure of an AC contactor is primarily caused by the electrical erosion that gradually accumulates on the surfaces of the contacts over time. This cumulative erosion

(*) Corresponding author.
E-mail addresses: C. Zhao (ORCID: 0009-0004-4447-335X) 1159732872@qq.com, S. Xiang (ORCID: 0000-0001-5647-0210) 2020070@hebut.edu.cn, F. Niu (ORCID: 0000-0003-2465-647X) niufeng@hebut.edu.cn, K. Li (ORCID: 0000-0002-3866-6700) likui@hebut.edu.cn

reduces the thickness of the contacts, eventually preventing them from closing properly. At this point, the AC contactor is considered failed. The electrical erosion mainly results from the arcing phenomenon between the contact pair, and its extent is typically quantified using the cumulative arcing Joule integral [7]. Hence, the cumulative arcing Joule integral between the contact pair of each phase is one of the most commonly used performance parameters, which reflects the health condition of an AC contactor [7–9]. When the cumulative arcing Joule integral between any pair of the three-phase contact pairs reaches a failure threshold, the AC contactor is considered to have failed [9].

The characteristic of multiple arcing modes can be explained in three aspects. Firstly, at the initial instant of a breaking process of an AC contactor, if the current flowing through a contact pair is sufficiently high, it creates the condition conducive to the thermal ionization between the contact pair. At this stage, an arc forms if the voltage is also high enough [10]. Thus, if the current and the voltage are sufficiently low at the initial instant of a breaking process, no arc will arise between the contact pair, leading to the arcing Joule integral being zero in the breaking process. Owing to the 120° phase difference between the currents/voltages of any two phases [7], there is at most one contact pair through which the current and voltage are close to zero at the initial moment of a breaking process. Hence, there can be at most one contact pair that does not experience arcing and has an arcing Joule integral being zero in the breaking process. Based on this, four arcing modes can be identified in a breaking process from the perspective of whether arcing is absent between any pair of contacts. In arcing modes I, II, and III, there is a single contact pair between which no arc arises. In arcing mode IV, all the three contact pairs suffer from the arcing phenomenon. Secondly, due to the arcing Joule integral being a nonlinear function of the phase angle of the current and the 120° phase difference between the currents of any two phases [7], the nonlinear correlation exists among the arcing Joule integrals of the phases experiencing arcing. Thirdly, since a sufficiently high current is a necessary condition for the arcing between a contact pair, and the arcing Joule integral is calculated based on the current, it can be deduced that the arcing Joule integral has a lower bound greater than zero. Furthermore, because an arc will extinguish when the current reaches zero [9], the duration of the arcing is limited, which implies that the arcing Joule integral also has an upper bound. Therefore, to accurately depict the degradation processes of AC contactors, it is essential to consider the characteristics of competing failure and multiple arcing modes. Notably, the characteristic of multiple arcing modes results in a complex degradation pattern, including zero degradation increments, bounded degradation increments, and nonlinear degradation correlation.

The RUL prediction for AC contactors has received much attention, with recent literature identifying three representative state-of-the-art methods: the highest degradation level (HDL) method, the average degradation level (ADL) method, and the model regression (MR) method. In the HDL method [9], the degradation data of the contact pair exhibiting the highest degradation level at the current time are used to reflect the degradation process of an AC contactor. The Wiener process model is adopted to capture this degradation process, followed by predicting the RUL of the AC contactor. In the ADL method [7], the average degradation level of the three-phase contact pairs is employed to quantify the performance state of an AC contactor. The Wiener process model is applied to model the evolution of the average degradation level, and it is then used to predict the RUL. In the MR method [8,11], regression models, such as the conditional density estimation model and the unitary regression model, are employed to capture the relationship between the degradation levels of the three-phase contact pairs and the RULs of AC contactors. Then, the RUL of an AC contactor is predicted using these models, which are trained based on the degradation data and actual RULs from other AC contactors.

The aforementioned methods present two issues. Firstly, both the HDL and ADL methods do not take into account multiple arcing modes, which means that they fail to consider zero degradation increments, bounded degradation increments, and nonlinear degradation correlation. As a result, these methods are unable to accurately capture the degradation of AC contactors, potentially compromising the precision of RUL prediction. Secondly, the MR method relies on prior data from other AC contactors. This could undermine the RUL prediction performance, as the discrepancy may exist between the degradation process of the AC contactor whose RUL needs to be predicted and the degradation processes of the ones

supplying the prior data. Such discrepancy can be caused by factors such as differing operating environments and inherent unit-to-unit variations [9].

Analyzing multiple dependent degradation processes is a hot topic in the reliability field. Existing studies primarily encompass machine learning methods and statistical modeling methods [12]. Machine learning methods leverage historical data to capture multiple dependent degradation processes. Such methods depend on an extensive amount of high-quality data to effectively train the model. However, in many real-world scenarios, acquiring sufficient degradation data is a challenging task, which limits the practical application of machine learning methods. Moreover, they lack the interpretability of degradation mechanism [13].

For statistical modeling methods, they can develop a degradation model by properly depicting degradation mechanism, and can be applied when the data size is not very large [14]. Statistical modeling methods typically involve two stages when modeling multiple dependent degradation processes. Firstly, each marginal degradation process is modeled using a stochastic process model, such as the Wiener process, gamma process, inverse Gaussian process, and Tweedie exponential dispersion process models [15,16]. Then, the correlation among the increments of the marginal degradation processes is captured using various correlation models, among which the multivariate normal distribution is usually employed due to its simplicity [17]. However, the multivariate normal distribution can only capture the linear correlation. To model the nonlinear correlation, models from the Archimedean copula family (e.g., Frank, Clayton, and Gumbel copulas) and the elliptical copula family (e.g., t and Gaussian copulas) are widely used [18,19]. Here, the Gaussian copula can be regarded as a special case of the t copula [20]. Notably, since a model from the Archimedean copula family has only a single model parameter, it may lack the flexibility to capture the nonlinear correlation among increments of more than two marginal degradation processes [21,22]. In comparison, a model from the elliptical copula family can more flexibly describe the nonlinear correlation among increments of any number of marginal degradation processes using the correlation matrix [23–25].

To the best of our knowledge, the existing methods of multiple dependent degradation processes modeling are unsuitable for AC contactors, as they fail to fully account for the unique degradation characteristics of AC contactors. These modeling methods are developed based on widely used degradation models, which typically assume that the degradation increments of each marginal degradation process range over the interval $(-\infty,+\infty)$ or $(0,+\infty)$, without considering the occurrence of zero and bounded degradation increments. Therefore, it is necessary to propose a novel degradation modeling method considering zero and bounded increments to provide a foundation for accurately predicting the RUL of AC contactors.

In this paper, we propose a novel RUL prediction method for AC contactors, considering multiple arcing modes with zero and bounded degradation increments, through a deep analysis of the arcing mechanism. The key contributions of this study are summarized as follows.

1) To fully reveal the characteristics of arcing Joule integrals, i.e., degradation increments, the physical model of the arcing Joule integral is derived through an analysis of the arcing mechanism. Using this model, the bounds of arcing Joule integrals are obtained by introducing critical breaking phase angles. Moreover, four arcing modes are identified according to the absence of arcing between any pair of contacts.
2) To effectively capture the evolution of the cumulative arcing Joule integral, the arcing mode similarity based discrete-time Markov chain model is first proposed to describe the transitions of the arcing modes. Then, the doubly truncated Tweedie exponential dispersion process model with zero increments is proposed to depict the degradation of a single-phase contact pair. Additionally, the t copula function is used to model the nonlinear degradation correlation among the three-phase contact pairs.
3) To accurately predict the RUL of an AC contactor, an analytical likelihood function is first derived, based on which the model parameters are updated as degradation data accumulates. Moreover, the truncated normal distribution is employed to model the randomness of the failure threshold, and it is updated through conditional probability analysis given increasing size of degradation

data. Subsequently, a Monte Carlo simulation based RUL prediction method is provided.

The rest of this paper is organized as follows. Section 2 analyzes the arcing mechanism. Section 3 details the main modeling assumptions. Section 4 shows the RUL prediction method. Section 5 displays the case study. Finally, Section 6 concludes the study.

2. Mechanism analysis

In this section, we theoretically derive the bounds of a nonzero arcing Joule integral. Then, we identify four arcing modes according to whether a pair of contacts exists between which no arc arises.

2.1. Arcing joule integral

An AC contactor has three pairs of contacts corresponding to phases A, B, and C, respectively. The contact pairs carry the three-phase current and voltage loads with a phase difference of 120° between any two phases [26]. Without loss of generality, we assume that the current between the contact pair of phase j for $j = A, B, C$ in an AC contactor at instant τ is expressed as $i_j(\tau) = \sqrt{2}I\sin\left(\tilde{\phi}_j(\tau)\right)$, where I is the root-mean-square current, and $\tilde{\phi}_j(\tau) = \omega\tau + \theta_j$ is the phase angle of $i_j(\tau)$ with the angular frequency ω and the phase shift θ_j.

We define $\phi_j(\tau) \in [0, \pi)$ as the transformed phase angle of the current between the contact pair of phase j by:

$$\phi_j(\tau) = \left|\tilde{\phi}_j(\tau) - \pi\left\lfloor\tilde{\phi}_j(\tau)/\pi\right\rfloor\right| \tag{1}$$

where $\left\lfloor\tilde{\phi}_j(\tau)/\pi\right\rfloor$ is the closest integer of $\tilde{\phi}_j(\tau)/\pi$ towards 0. Then, we rewrite $i_j(\tau)$ as:

$$\begin{aligned} i_j(\tau) &= \sqrt{2}I\sin\left(\tilde{\phi}_j(\tau)\right) \\ &= \delta\left(\sin\left(\tilde{\phi}_j(\tau)\right)\right)\sqrt{2}I\sin\left(\phi_j(\tau)\right) \\ &= \delta\left(\sin\left(\tilde{\phi}_j(\tau)\right)\right)\sqrt{2}I\sin\left(\left|\tilde{\phi}_j(\tau) - \pi\left\lfloor\tilde{\phi}_j(\tau)/\pi\right\rfloor\right|\right) \end{aligned} \tag{2}$$

in which:

$$\delta\left(\sin\left(\tilde{\phi}_j(\tau)\right)\right) = \begin{cases} -1, & \sin\left(\tilde{\phi}_j(\tau)\right) < 0 \\ 1, & \sin\left(\tilde{\phi}_j(\tau)\right) \geq 0 \end{cases} \tag{3}$$

According to (1), the original phase angle $\tilde{\phi}_j(\tau) \in (-\infty, +\infty)$ is transformed into $\phi_j(\tau) \in [0, \pi)$. This transformation aims to simplify the calculation of the arcing Joule integral by utilizing the periodicity of $i_j^2(\tau)$ with a period length of π. Let $\phi_j(\tau_b)$ denote the transformed phase angle of the current between the contact pair of phase j at the initial instant τ_b of a breaking process of an AC contactor. For simplicity, $\phi_j(\tau_b)$ is referred to as the breaking phase angle of phase j. A graphical representation of the current is given in Fig. 1(a), where the normalized current is calculated by $i_j(\tau_b)/\sqrt{2}I$.

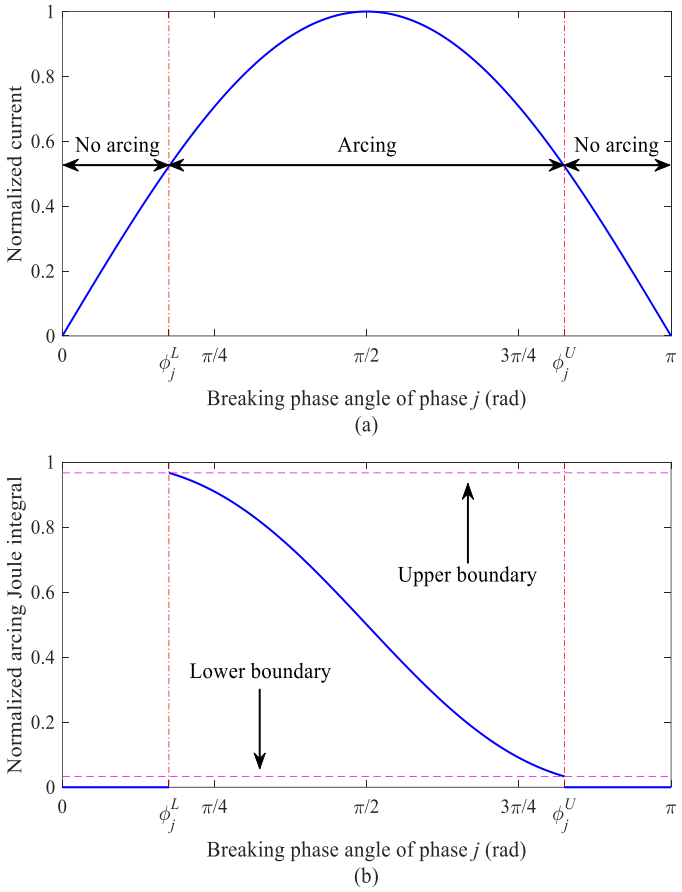

Figure 1. (a) Normalized current and (b) normalized arcing Joule integral between the contact pair of phase j.

Since a contact pair can be treated as a resistor, the phase difference between the current and voltage carried by the contact pair is zero. Thus, when $\phi_j(\tau_b)$ is close to 0 or π, both the current and voltage carried by the contact pair are very small, preventing the contact pair from suffering an arc, according to the arcing mechanism. To reflect the extent to which $\phi_j(\tau_b)$ is close to 0 or π, we introduce two critical breaking phase angles $\phi_j^L \in [0, \pi/2]$ and $\phi_j^U \in [\pi/2, \pi)$. We consider them as the lower and upper bounds of the arcing phase angle that is the breaking phase angle with which an arc can be generated. If $\phi_j(\tau_b) \in \left[\phi_j^L, \phi_j^U\right]$, then the current and the voltage are assumed to be large enough to cause an arc. Otherwise, if $\phi_j(\tau_b) \in \left[0, \phi_j^L\right) \cup \left(\phi_j^U, \pi\right)$, then the current and the voltage are assumed to be sufficiently low such that no arc can arise.

The cumulative arcing Joule integral is the most commonly used performance parameter for an AC contactor. An arcing

Joule integral equal to zero indicates that no arcing occurs [9]. The arcing Joule integral between the contact pair of phase j for $j = A, B, C$ in a breaking process is given by [7]:

$$x_j = \int_{\tau_b}^{\tau_b+\tau_{j,arc}} i_j^2(\tau)\,\mathrm{d}\tau \tag{4}$$

where $\tau_{j,arc}$ is the duration of arcing.

If $\phi_j(\tau_b) \in [0, \phi_j^L) \cup (\phi_j^U, \pi)$, then there is no arc between the contact pair of phase j, leading to $\tau_{j,arc} = 0$ and hence $x_j = 0$.

If $\phi_j(\tau_b) \in [\phi_j^L, \phi_j^U]$, then an arc arises between the contact pair at τ_b and extinguishes at $\tau_b + \tau_{j,arc}$. By substituting (2) into (4), we have:

$$\begin{aligned} x_j &= \int_{\tau_b}^{\tau_b+\tau_{j,arc}} \left[\delta\left(\sin\left(\tilde{\phi}_j(\tau)\right)\right)\sqrt{2}I\sin\left(\phi_j(\tau)\right)\right]^2 \mathrm{d}\tau \\ &= I^2 \int_{\tau_b}^{\tau_b+\tau_{j,arc}} \left[1-\cos\left(2\phi_j(\tau)\right)\right]\mathrm{d}\tau \\ &= \frac{I^2}{\omega}\left[\phi_j(\tau) - \frac{1}{2}\sin\left(2\phi_j(\tau)\right)\right]\Big|_{\tau=\tau_b}^{\tau=\tau_b+\tau_{j,arc}} \\ &= \frac{I^2}{\omega}\left[\pi - \phi_j(\tau_b) + \frac{1}{2}\sin\left(2\phi_j(\tau_b)\right)\right] \end{aligned} \tag{5}$$

where the second equation is derived with the aid of the trigonometric identity, and $\phi_j(\tau_b + \tau_{j,arc}) = \pi$ holds in the last equation because an arc extinguishes when the current reaches zero [9].

In summary, we can express x_j by:

$$x_j = \begin{cases} 0, \phi_j(\tau_b) \in [0, \phi_j^L) \cup (\phi_j^U, \pi), \\ \frac{I^2}{\omega}\left[\pi - \phi_j(\tau_b) + \frac{1}{2}\sin\left(2\phi_j(\tau_b)\right)\right], \phi_j(\tau_b) \in [\phi_j^L, \phi_j^U] \end{cases} \tag{6}$$

where $j = A, B, C$.

The following two potential cases in a breaking process are illustrated by (6). Firstly, when $\phi_j(\tau_b) \in [0, \phi_j^L) \cup (\phi_j^U, \pi)$, the arcing Joule integral is zero. Secondly, when $\phi_j(\tau_b) \in [\phi_j^L, \phi_j^U]$, the arcing Joule integral between the contact pair of phase j is a positive value, with the upper bound $U(\phi_j^L)$ and the lower bound $L(\phi_j^U)$, given by:

$$\begin{cases} U(\phi_j^L) = \omega^{-1}I^2\{\pi - \phi_j^L + 2^{-1}\sin(2\phi_j^L)\} \\ L(\phi_j^U) = \omega^{-1}I^2\{\pi - \phi_j^U + 2^{-1}\sin(2\phi_j^U)\} \end{cases} \tag{7}$$

A graphical representation of the arcing Joule integral is given in Fig. 1(b), where the normalized arcing Joule integral is calculated by $x_j\omega/(\pi I^2)$.

2.2. Four arcing modes

Owing to the 120° phase difference between the currents/voltages of any two phases [7], there is at most one contact pair through which the current and voltage are close to zero at the initial moment of a breaking process. Hence, there can be at most one contact pair that does not experience arcing and has an arcing Joule integral being zero in the breaking process. Based on this, from the perspective of whether arcing is absent between any pair of contacts, we identify the following four potential arcing modes for an AC contactor in a breaking process.

Arcing mode I: No arc arises between the contact pair of phase A, whereas arcs arise between the contact pair of phase B and between the contact pair of phase C.

Arcing mode II: No arc arises between the contact pair of phase B, whereas arcs arise between the contact pair of phase A and between the contact pair of phase C.

Arcing mode III: No arc arises between the contact pair of phase C, whereas arcs arise between the contact pair of phase A and between the contact pair of phase B.

Arcing mode IV: Arcs arise between the contact pair of phase A, between the contact pair of phase B, and between the contact pair of phase C.

Let $M(t) = m$ for $m = \mathrm{I}, \mathrm{II}, \mathrm{III}, \mathrm{IV}$ denote the arcing mode that an AC contactor is in during the breaking process of the t-th operation cycle. Here, the t-th operation cycle includes the t-th requested closing and subsequent t-th requested breaking of the AC contactor.

3. Modeling assumptions

3.1. Arcing mode evolution model

We propose the arcing mode similarity based discrete-time Markov chain model, which depicts the transition characteristic of the four arcing modes. Specifically, we define the transition probability matrix from the t-th operation cycle to the $(t+1)$-th operation cycle as:

$$\boldsymbol{P}_t = \begin{bmatrix} P_{\mathrm{I,I}} & P_{\mathrm{I,II}} & P_{\mathrm{I,III}} & P_{\mathrm{I,IV}} = 1 - \sum_{m=\mathrm{I}}^{\mathrm{III}} P_{\mathrm{I},m} \\ P_{\mathrm{II,I}} & P_{\mathrm{II,II}} & P_{\mathrm{II,III}} & P_{\mathrm{II,IV}} = 1 - \sum_{m=\mathrm{I}}^{\mathrm{III}} P_{\mathrm{II},m} \\ P_{\mathrm{III,I}} & P_{\mathrm{III,II}} & P_{\mathrm{III,III}} & P_{\mathrm{III,IV}} = 1 - \sum_{m=\mathrm{I}}^{\mathrm{III}} P_{\mathrm{III},m} \\ P_{\mathrm{IV,I}}(t) & P_{\mathrm{IV,II}}(t) & P_{\mathrm{IV,III}}(t) & P_{\mathrm{IV,IV}}(t) = 1 - \sum_{m=\mathrm{I}}^{\mathrm{III}} P_{\mathrm{IV},m}(t) \end{bmatrix} \tag{8}$$

where $P_{n,m}$ is the transition probability from arcing mode n in the t-th operation cycle to arcing mode m in the $(t+1)$-th operation cycle, and it is a constant for $n = \mathrm{I}, \mathrm{II}, \mathrm{III}$ and $m = \mathrm{I}, \mathrm{II}, \mathrm{III}, \mathrm{IV}$. However, we assume that if the AC contactor is in arcing mode IV in the t-th operation cycle, the transition probability $P_{\mathrm{IV},m}(t)$ for $m = \mathrm{I}, \mathrm{II}, \mathrm{III}, \mathrm{IV}$ is a function of t that is determined according to the arcing mode similarity. We define

$P_{\mathrm{IV},m}(t)$ as:

$$P_{IV,m}(t) = \sum_{n=I}^{III} W_n(t) P_{n,m} \tag{9}$$

where $W_n(t)$ is the proposed arcing mode similarity index. It aims to measure the similarity between the actual arcing Joule integrals of the three-phase contact pairs in the t-th operation cycle and the imaginary arcing Joule integrals of the three-phase contact pairs, which are obtained by imagining that the AC contactor is in arcing model n in the t-th operation cycle for $n = \mathrm{I}, \mathrm{II}, \mathrm{III}$.

We specify $W_n(t)$ as follows. Let $X_{j,n}(t)$ be a random variable denoting the imaginary arcing Joule integral of phase j in arcing mode n within the t-th operation cycle. Let $\boldsymbol{X}_{\mathrm{I}} = \left(0, X_{B,\mathrm{I}}(t), X_{C,\mathrm{I}}(t)\right)'$, $\boldsymbol{X}_{\mathrm{II}} = \left(X_{A,\mathrm{II}}(t), 0, X_{C,\mathrm{II}}(t)\right)'$, and $\boldsymbol{X}_{\mathrm{III}} = \left(X_{A,\mathrm{III}}(t), X_{B,\mathrm{III}}(t), 0\right)'$ denote the random vectors of the imaginary arcing Joule integrals in arcing modes I, II, and III, respectively. According to [27], the elastic probability model can flexibly measure the similarity between two vectors. Therefore, to construct $W_n(t)$, we first define the conditional arcing mode similarity index $\widetilde{W}_n(t|\boldsymbol{X}_{\mathrm{I}}, \boldsymbol{X}_{\mathrm{II}}, \boldsymbol{X}_{\mathrm{III}})$ by:

$$\widetilde{W}_n(t|\boldsymbol{X}_{\mathrm{I}}, \boldsymbol{X}_{\mathrm{II}}, \boldsymbol{X}_{\mathrm{III}}) = \frac{\exp\left(-\frac{D_n(t)}{\varepsilon}\right)}{\sum_{m=\mathrm{I}}^{\mathrm{III}} \exp\left(-\frac{D_m(t)}{\varepsilon}\right)} \tag{10}$$

where ε is the elastic factor, which is the parameter to be estimated, and $D_n(t)$ is the Euclidean distance between the actual arcing Joule integrals and the imaginary arcing Joule integrals, expressed as:

$$D_n(t) = \|\boldsymbol{x}(t) - \boldsymbol{X}_n\|_2 \tag{11}$$

in which $\|\cdot\|_2$ is the Euclidean norm, and $\boldsymbol{x}(t) = \left(x_A(t), x_B(t), x_C(t)\right)'$ with $x_j(t)$ being the actual arcing Joule integral observation of phase j in the t-th operation cycle.

Since there are three random vectors $\boldsymbol{X}_{\mathrm{I}}$, $\boldsymbol{X}_{\mathrm{II}}$, and $\boldsymbol{X}_{\mathrm{III}}$ in $\widetilde{W}_n(t|\boldsymbol{X}_{\mathrm{I}}, \boldsymbol{X}_{\mathrm{II}}, \boldsymbol{X}_{\mathrm{III}})$, we define the arcing mode similarity index $W_n(t)$ as the expectation of $\widetilde{W}_n(t|\boldsymbol{X}_{\mathrm{I}}, \boldsymbol{X}_{\mathrm{II}}, \boldsymbol{X}_{\mathrm{III}})$, which yields:

$$\begin{aligned} W_n(t) &= E_{\boldsymbol{X}_I, \boldsymbol{X}_{II}, \boldsymbol{X}_{III}}\left(\widetilde{W}_n(t|\boldsymbol{X}_I, \boldsymbol{X}_{II}, \boldsymbol{X}_{III})\right) \\ &= E_{\boldsymbol{X}_I, \boldsymbol{X}_{II}, \boldsymbol{X}_{III}}\left(\frac{exp\left(-\frac{\|x(t)-X_n\|_2}{\varepsilon}\right)}{\sum_{m=I}^{III} exp\left(-\frac{\|x(t)-X_m\|_2}{\varepsilon}\right)}\right) \end{aligned} \tag{12}$$

By substituting (9) into (8) and combining (12) with (8), the arcing mode similarity based transition probability matrix is finally expressed as:

$$\boldsymbol{P}_t = \begin{bmatrix} P_{\mathrm{I,I}} & P_{\mathrm{I,II}} & P_{\mathrm{I,III}} & 1 - \sum_{m=\mathrm{I}}^{\mathrm{III}} P_{\mathrm{I},m} \\ P_{\mathrm{II,I}} & P_{\mathrm{II,II}} & P_{\mathrm{II,III}} & 1 - \sum_{m=\mathrm{I}}^{\mathrm{III}} P_{\mathrm{II},m} \\ P_{\mathrm{III,I}} & P_{\mathrm{III,II}} & P_{\mathrm{III,III}} & 1 - \sum_{m=\mathrm{I}}^{\mathrm{III}} P_{\mathrm{III},m} \\ \sum_{n=\mathrm{I}}^{\mathrm{III}} W_n(t) P_{n,\mathrm{I}} & \sum_{n=\mathrm{I}}^{\mathrm{III}} W_n(t) P_{n,\mathrm{II}} & \sum_{n=\mathrm{I}}^{\mathrm{III}} W_n(t) P_{n,\mathrm{III}} & 1 - \sum_{m=\mathrm{I}}^{\mathrm{III}} \sum_{n=\mathrm{I}}^{\mathrm{III}} W_n(t) P_{n,m} \end{bmatrix} \tag{13}$$

where:

$$\begin{aligned} W_n(t) = \int_{L(\phi_A^L)}^{U(\phi_A^L)} \int_{L(\phi_A^U)}^{U(\phi_A^U)} \int_{L(\phi_B^L)}^{U(\phi_B^L)} \int_{L(\phi_B^U)}^{U(\phi_B^U)} \int_{L(\phi_C^L)}^{U(\phi_C^L)} \int_{L(\phi_C^U)}^{U(\phi_C^U)} \\ \left\{ \frac{\exp\left(-\frac{\|x(t)-X_n\|_2}{\varepsilon}\right)}{\sum_{m=\mathrm{I}}^{\mathrm{III}} \exp\left(-\frac{\|x(t)-X_m\|_2}{\varepsilon}\right)} g_{B,C}\left(u_{B,\mathrm{I}}, u_{C,\mathrm{I}}\right) \right. \\ \left. \times g_{A,C}\left(u_{A,\mathrm{II}}, u_{C,\mathrm{II}}\right) g_{A,B}\left(u_{A,\mathrm{III}}, u_{B,\mathrm{III}}\right) \right\} \\ \times du_{A,\mathrm{II}} du_{A,\mathrm{III}} du_{B,\mathrm{I}} du_{B,\mathrm{III}} du_{C,\mathrm{I}} du_{C,\mathrm{II}}, \end{aligned} \tag{14}$$

in which $\boldsymbol{X}_{\mathrm{I}} = \left(0, u_{B,\mathrm{I}}, u_{C,\mathrm{I}}\right)'$, $\boldsymbol{X}_{\mathrm{II}} = \left(u_{A,\mathrm{II}}, 0, u_{C,\mathrm{II}}\right)'$, and $\boldsymbol{X}_{\mathrm{III}} = \left(u_{A,\mathrm{III}}, u_{B,\mathrm{III}}, 0\right)'$. Furthermore, $g_{B,C}\left(u_{B,\mathrm{I}}, u_{C,\mathrm{I}}\right)$, $g_{A,C}\left(u_{A,\mathrm{II}}, u_{C,\mathrm{II}}\right)$, and $g_{A,B}\left(u_{A,\mathrm{III}}, u_{B,\mathrm{III}}\right)$ are the joint probability density functions (PDFs) of $\left(X_{B,\mathrm{I}}(t), X_{C,\mathrm{I}}(t)\right)'$, $\left(X_{A,\mathrm{II}}(t), X_{C,\mathrm{II}}(t)\right)'$, and $\left(X_{A,\mathrm{III}}(t), X_{B,\mathrm{III}}(t)\right)'$, respectively. These joint PDFs are specified later in Subsection 3.3.

Additionally, we assume that the initial probability P_m of the AC contactor being in arcing mode m within the first operation cycle is a constant for $m = \mathrm{I}, \mathrm{II}, \mathrm{III}, \mathrm{IV}$. Then, we can specify the arcing mode similarity based discrete-time Markov chain model by combining the initial probability P_m and the transition probability matrix $\boldsymbol{P}_t$ in (13).

3.2. Single-phase contact pair degradation model

The Tweedie exponential dispersion process (TEDP) model is usually utilized in reliability research due to its flexibility in modeling various degradation processes, including Wiener, gamma, and inverse Gaussian process models as special cases [28,29]. Nevertheless, the TEDP model is unsuitable for depicting the degradation process of the cumulative arcing Joule integral between the contact pair of a phase in an AC contactor. As explained in Subsection 2.1, if no arcing occurs between the contact pair of phase j for $j = A, B, C$ in the t-th operation cycle, the arcing Joule integral $X_j(t)$ is equal to 0; if arcing occurs, $X_j(t)$ is bounded above by $U(\phi_j^L)$ and below by $L(\phi_j^U)$. Thus, a degradation model with zero and bounded increments is required. However, the increment of the TEDP model is a continuous random variable in the interval $(0, +\infty)$ or $(-\infty, +\infty)$. As a result, the TEDP model cannot accurately capture the evolution process of the cumulative arcing Joule integral.

To address the above issue, we propose the doubly truncated TEDP model with zero increments as the single-phase contact pair degradation model. For the degradation process of the cumulative arcing Joule integral $Y_j(t)$ between the contact pair of phase j, we define the doubly truncated TEDP model with

zero increments as:

$$Y_j(t) = \sum_{\xi=1}^{t} X_j(\xi) \tag{15}$$

where t is the operation cycle number, and $X_j(\xi)$ is the arcing Joule integral between the contact pair of phase j for $j = A, B, C$ in the ξ-th operation cycle, satisfying:

$$\begin{cases} \Pr\{X_j(t) = 0 | t = 1\} = P_m, \\ \Pr\{X_j(t) = 0 | M(t-1) = n, t > 1\} = P_{n,m}, \\ \Pr\{X_j(t) = 0 | M(t-1) = \mathrm{IV}, t > 1\} \\ = P_{\mathrm{IV},m}(t-1) = \sum_{n=\mathrm{I}}^{\mathrm{III}} W_n(t-1) P_{n,m}, \\ \Pr\{X_j(t) \le x_j | M(t) \ne m\} = G_j(x_j), \end{cases} \tag{16}$$

where $M(t) = m$ denotes that the AC contactor is in arcing mode m during the t-th operation cycle, and $n, m = \mathrm{I}, \mathrm{II}, \mathrm{III}$. Moreover, if $m = \mathrm{I}$, then $j = A$; if $m = \mathrm{II}$, then $j = B$; and if $m = \mathrm{III}$, then $j = C$. The first three equations describe the randomness of whether no arc arises between the contact pair of phase j in the t-th operation cycle. The last equation depicts the randomness in the magnitude of the arcing Joule integral when an arc arises. $G_j(x_j)$ is the cumulative distribution function (CDF) of $X_j(t) | M(t) \ne m$, derived as:

$$\begin{aligned} G_j(x_j) &= \int_{L(\phi_j^U)}^{x_j} g_i(u_j) \mathrm{d}u_j \\ &\approx \left(\int_{L(\phi_j^U)}^{U(\phi_j^L)} f_j(u_j) \mathrm{d}u_j \right)^{-1} \int_{L(\phi_j^U)}^{x_j} f_j(u_j) \mathrm{d}u_j \\ &= \left(\int_{L(\phi_j^U)}^{U(\phi_j^L)} \sqrt{\frac{\lambda_j}{2\pi \left(t^{\delta_j} - (t-1)^{\delta_j}\right)^{1-\rho_j} (u_j)^{\rho_j}}} \right. \\ &\quad \left. \times \exp\left\{ -\frac{\lambda_j \left(t^{\delta_j} - (t-1)^{\delta_j}\right)}{2} d_j(u_j) \right\} \mathrm{d}u_j \right)^{-1} \\ &\quad \times \int_{L(\phi_j^U)}^{x_j} \sqrt{\frac{\lambda_j}{2\pi \left(t^{\delta_j} - (t-1)^{\delta_j}\right)^{1-\rho_j} (u_j)^{\rho_j}}} \\ &\quad \times \exp\left\{ -\frac{\lambda_j \left(t^{\delta_j} - (t-1)^{\delta_j}\right)}{2} d_j(u_j) \right\} \mathrm{d}u_j, \end{aligned} \tag{17}$$

where $g_j(u_j)$ is the PDF of $X_j(t) | M(t) \ne m$, $f_j(u_j)$ is the approximated PDF of the increment of the TEDP model [30], λ_j, δ_j, ρ_j, and η_j are the model parameters, and $d_j(u_j)$ is written as:

$$d_j(u_j) = \begin{cases} \left\{ \frac{u_j}{\left[t^{\delta_j} - (t-1)^{\delta_j}\right]} - \eta_j \right\}^2, & \rho_j = 0, \\ 2\left\{ \frac{u_j}{t^{\delta_j} - (t-1)^{\delta_j}} \ln\left(\frac{u_j}{\eta_i \left[t^{\delta_j} - (t-1)^{\delta_j}\right]} \right) \right. & \rho_j = 1, \\ \left. - \left(\frac{u_j}{t^{\delta_j} - (t-1)^{\delta_j}} - \eta_j \right) \right\}, & \\ 2\left\{ \ln\left(\frac{\eta_j \left[t^{\delta_j} - (t-1)^{\delta_j}\right]}{u_i} \right) + \frac{u_j}{\eta_j \left[t^{\delta_j} - (t-1)^{\delta_j}\right]} - 1 \right\}, & \rho_j = 2, \\ 2\left\{ \left[\max\left(\frac{u_j}{t^{\delta_j} - (t-1)^{\delta_j}}, 0 \right) \right]^{2-\rho_j} (1-\rho_j)^{-1} (2-\rho_j)^{-1} \right. & \\ \left. - \frac{\eta_j^{1-\rho_j} u_j}{(1-\rho_j)\left[t^{\delta_j} - (t-1)^{\delta_j}\right]} + \frac{\eta_j^{2-\rho_j}}{2-\rho_j} \right\}, & \rho_j \ne 0,1,2. \end{cases} \tag{18}$$

3.3. Three-phase contact pair degradation model

Nonlinear correlation exists among the arcing Joule integrals of the contact pairs that suffer from arcs in a breaking process. This nonlinear correlation is explained as below. Under the three-phase current condition, the original phase angles exhibit a phase difference of 120° between any two phases. These original phase angles are nonlinearly transformed into the breaking phase angles according to (1), resulting in the nonlinear correlation among the breaking phase angles. Meanwhile, it can be observed from (6) that the arcing Joule integral is a nonlinear function of the breaking phase angle.

Based on the models proposed in Subsections 3.1 and 3.2, we further model the performance evolution process of an AC contactor by capturing the correlation among the arcing Joule integrals of the three-phase contact pairs using the t copula function. This copula function is widely employed to describe the nonlinear correlation among multiple random variables in reliability studies, and it can flexibly depict the nonlinear correlation between any two of all the random variables using the correlation matrix [23,24].

We define the three-phase contact pair degradation model as follows:

$$Y_A(t) = \sum_{\xi=1}^{t} X_A(\xi), Y_B(t) = \sum_{\xi=1}^{t} X_B(\xi), Y_C(t) = \sum_{\xi=1}^{t} X_C(\xi) \tag{19}$$

where the randomness and correlation characteristics of $X_A(t)$, $X_B(t)$, and $X_C(t)$ are described by (20) and (23).

For arcing mode m, $m = \mathrm{I}, \mathrm{II}, \mathrm{III}$, we assume that:

$$\begin{cases} \Pr\{X_j(t) = 0 | t = 1\} = P_m, \\ \Pr\{X_j(t) = 0 | M(t-1) = n, t > 1\} = P_{n,m}, \\ \Pr\{X_j(t) = 0 | M(t-1) = \mathrm{IV}, t > 1\} \\ = P_{\mathrm{IV},m}(t-1) = \sum_{n=\mathrm{I}}^{\mathrm{III}} W_n(t-1) P_{n,m}, \\ \Pr\{X_k(t) \le x_k, X_l(t) \le x_l | M(t) = m\} \\ = \int_{L(\phi_k^U)}^{x_k} \int_{L(\phi_l^U)}^{x_l} g_{k,l}(u_k, u_l) \, \mathrm{d}u_k \mathrm{d}u_l, \end{cases} \tag{20}$$

where $n = \mathrm{I}, \mathrm{II}, \mathrm{III}$. Moreover, if $m = \mathrm{I}$, then $j = A$, $k = B$, and $l = C$; if $m = \mathrm{II}$, then $j = B$, $k = A$, and $l = C$; if $m = \mathrm{III}$, then $j = C$, $k = A$, and $l = B$. The first three equations describe the randomness of whether no arc arises between the contact pair of phase j, with arcs arising for the contact pairs of the other two phases, in the t-th operation cycle. The last equation depicts the randomness in the magnitudes of the arcing Joule integrals for the two contact pairs when arcs arise in them. $g_{k,l}(x_k, x_l)$ is the joint PDF of $X_k(t), X_l(t) | M(t) = m$.

Based on the t copula function, $g_{k,l}(x_k, x_l)$ is given by:

$$g_{k,l}(x_k,x_l)=\frac{\Gamma\left(\frac{\nu+2}{2}\right)}{\nu\pi\Gamma\left(\frac{\nu}{2}\right)|\boldsymbol{\Sigma}_{k,l}|^{\frac{1}{2}}}\left(1+\frac{1}{\nu}\mathbf{x}_{k,l}'\boldsymbol{\Sigma}_{k,l}^{-1}\mathbf{x}_{k,l}\right)^{-\frac{\nu+2}{2}}\times\left\{\zeta_\nu\left(t_\nu^{-1}\left(G_k(x_k)\right)\right)\zeta_\nu\left(t_\nu^{-1}\left(G_l(x_l)\right)\right)\right\}^{-1}\times g_k(x_k)g_l(x_l), \quad (21)$$

where $\Gamma(\cdot)$ is the gamma function, $\nu>2$ is the degrees of freedom, $\zeta_\nu(\cdot)$ and $t_\nu^{-1}(\cdot)$ are respectively the PDF and quantile function of the univariate standard t distribution with ν degrees of freedom, and $\mathbf{x}_{k,l}$ and $\boldsymbol{\Sigma}_{k,l}$ are expressed as:

$$\begin{cases}\mathbf{x}_{k,l}=\left[t_\nu^{-1}\left(G_k(x_k)\right),t_\nu^{-1}\left(G_l(x_l)\right)\right]'\\ \boldsymbol{\Sigma}_{k,l}=\begin{bmatrix}1 & \rho_{k,l}\\ \rho_{k,l} & 1\end{bmatrix}\end{cases} \quad (22)$$

in which $\rho_{k,l}$ is the correlation coefficient and $\boldsymbol{\Sigma}_{k,l}$ is the correlation matrix.

For arcing mode IV, we assume that:

$$\begin{cases}\Pr\{X_A(t)\neq 0,X_B(t)\neq 0,X_C(t)\neq 0|t=1\}=P_{\mathrm{IV}},\\ \Pr\{X_A(t)\neq 0,X_B(t)\neq 0,X_C(t)\neq 0|M(t-1)=n,t>1\}\\ =P_{n,\mathrm{IV}},\\ \Pr\{X_A(t)\neq 0,X_B(t)\neq 0,X_C(t)\neq 0|M(t-1)=\mathrm{IV},t>1\}\\ =P_{\mathrm{IV},\mathrm{IV}}(t-1)=\sum_{n=\mathrm{I}}^{\mathrm{III}}W_n(t-1)P_{n,\mathrm{IV}},\\ \Pr\{X_A(t)\leq x_A,X_B(t)\leq x_B,X_C(t)\leq x_C(t)|M(t)=\mathrm{IV}\}\\ =\int_{L(\phi_A^U)}^{x_A}\int_{L(\phi_B^U)}^{x_B}\int_{L(\phi_C^U)}^{x_C}g_{A,B,C}(u_A,u_B,u_C)\,du_Adu_Bdu_C,\end{cases} \quad (23)$$

where $n=\mathrm{I},\mathrm{II},\mathrm{III}$. The first three equations describe the randomness of whether arcs simultaneously arise for the three-phase contact pairs in the t-th operation cycle. The last equation depicts the randomness in the magnitudes of the arcing Joule integrals of the three-phase contact pairs when arcs arise in them. $g_{A,B,C}(x_A,x_B,x_C)$ is the joint PDF of $X_A(t),X_B(t),X_C(t)|M(t)=\mathrm{IV}$. Based on the t copula function, $g_{A,B,C}(x_A,x_B,x_C)$ is represented by:

$$g_{A,B,C}(x_A,x_B,x_C)=\frac{\Gamma\left(\frac{\nu+3}{2}\right)\left(1+\frac{1}{\nu}\mathbf{x}_{A,B,C}'\boldsymbol{\Sigma}_{A,B,C}^{-1}\mathbf{x}_{A,B,C}\right)^{-\frac{\nu+3}{2}}}{\nu^{\frac{3}{2}}\pi^{\frac{3}{2}}\Gamma\left(\frac{\nu}{2}\right)|\boldsymbol{\Sigma}_{A,B,C}|^{\frac{1}{2}}}\times\left\{\zeta_\nu\left(t_\nu^{-1}\left(G_A(x_A)\right)\right)\times\zeta_\nu\left(t_\nu^{-1}\left(G_B(x_B)\right)\right)\times\zeta_\nu\left(t_\nu^{-1}\left(G_C(x_C)\right)\right)\right\}^{-1}\times g_A(x_A)g_B(x_B)g_C(x_C), \quad (24)$$

in which $\mathbf{x}_{A,B,C}$ and $\boldsymbol{\Sigma}_{A,B,C}$ are given by:

$$\begin{cases}\mathbf{x}_{A,B,C}=\left[t_\nu^{-1}\left(G_A(x_A)\right),t_\nu^{-1}\left(G_B(x_B)\right),t_\nu^{-1}\left(G_C(x_C)\right)\right]'\\ \boldsymbol{\Sigma}_{A,B,C}=\begin{bmatrix}1 & \rho_{A,B} & \rho_{A,C}\\ \rho_{A,B} & 1 & \rho_{B,C}\\ \rho_{A,C} & \rho_{B,C} & 1\end{bmatrix}\end{cases} \quad (25)$$

3.4. Failure threshold distribution

The failure threshold of a contact pair can be considered to be the lowest cumulative arcing Joule integral with which poor connectivity or failure to close occurs for the contact pair. The failure thresholds for the contact pairs of different phases across different AC contactors may not be identical due to heterogeneity incurred by factors such as material inconsistencies and manufacturing process instabilities [9].

Let D_j denote the failure threshold of the contact pair of phase j in an AC contactor for $j=A,B,C$. We assume that D_j independently and identically follows a normal distribution with mean μ_D and variance σ_D^2, referred to as $D_j\sim N(\mu_D,\sigma_D^2)$. Furthermore, the model parameter vector $\boldsymbol{\theta}_D=(\mu_D,\sigma_D^2)'$ is estimated using the maximum likelihood estimation method detailed in Appendix-A.

4. RUL Prediction

The overall framework of the proposed RUL prediction method is illustrated in Fig. 2. This framework mainly consists of three parts.

a) Degradation modeling based on arcing mechanism analysis and the degradation characteristics of AC contactors, as detailed in Section 3.

b) Model updating for the degradation model and the failure threshold distribution, as presented in Subsection 4.1.

c) Monte Carlo simulation based RUL prediction, as described in Subsection 4.2.

4.1. Model updating

1) Degradation Model Parameter Estimates Updating: In this section, we derive the likelihood function to update the parameter estimates in the proposed three-phase contact pair degradation model as the accumulation of degradation data.

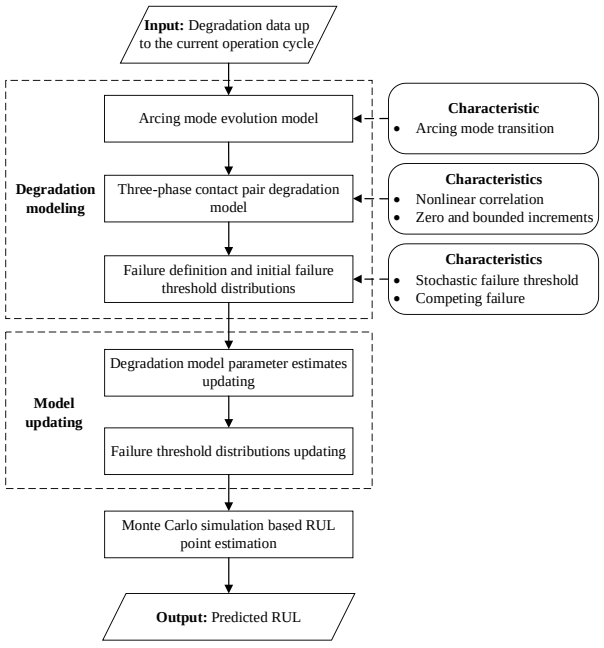

Figure 2. Flowchart of the proposed RUL prediction method.

Consider that the current operation cycle is the t_k-th one. Let $x_j(t)$ and $y_j(t) = \sum_{\xi=1}^{t} x_j(\xi)$ for $j = A, B, C$ represent the respective observations of the arcing Joule integral and cumulative arcing Joule integral between the contact pair of phase j in the t-th operation cycle. Moreover, let $t_l^{n,m}$ represent the operation cycle in which the AC contactor is in arcing mode n and after which the AC contactor is in arcing mode m. Additionally, the superscript l indicates the l-th such operation cycle for $l = 1,2,\cdots,k_{n,m}$, where $k_{n,m}$ is the total number satisfying $\sum_{n=\mathrm{I}}^{\mathrm{IV}} \sum_{m=\mathrm{I}}^{\mathrm{IV}} k_{n,m} = t_k - 1$. Then, the relationship between $x_j(t)$ and $x_j(t_l^{n,m})$ can be expressed as:

$$\begin{aligned}\{x_j(t), t = 1,2,\cdots,t_k\} = \underbrace{\cup_{n=\mathrm{I}}^{\mathrm{IV}} \cup_{m=\mathrm{I}}^{\mathrm{IV}} \{x_j(t_l^{n,m}), l = 1,2,\cdots,k_{n,m}\}}_{S_{j,1}} \\ \cup \underbrace{\{x_j(t_k)\}}_{S_{j,2}} = S_{j,1} \cup S_{j,2}\end{aligned} \tag{26}$$

where $j = A, B, C$.

The realization of the arcing mode evolution process can be obtained based on all the observed data $S_{j,1}$ and $S_{j,2}$ for $j = A, B, C$, according to the identification of the four arcing modes in Subsection 2.2. Using (13), the probability of this realization is derived by:

$$\begin{aligned}l_1(\boldsymbol{\theta}) = \prod_{n=\mathrm{I}}^{\mathrm{III}} \left\{ \left(1 - \sum_{m=\mathrm{I}}^{\mathrm{III}} P_{n,m}\right)^{k_{n,\mathrm{IV}}} \prod_{m=\mathrm{I}}^{\mathrm{III}} P_{n,m}^{k_{n,m}} \right\} \\ \times \prod_{l=1}^{k_{\mathrm{IV},\mathrm{IV}}} \left\{1 - \sum_{m=\mathrm{I}}^{\mathrm{III}} \sum_{n=\mathrm{I}}^{\mathrm{III}} W_n\left(t_l^{\mathrm{IV},\mathrm{IV}}\right) P_{n,m}\right\} \\ \times \prod_{m=\mathrm{I}}^{\mathrm{III}} \left\{ \prod_{l=1}^{k_{\mathrm{IV},m}} \sum_{n=\mathrm{I}}^{\mathrm{III}} W_n\left(t_l^{\mathrm{IV},m}\right) P_{n,m} \right\}\end{aligned} \tag{27}$$

where $\boldsymbol{\theta}$ is the vector of all the parameters in the proposed three-phase contact pair degradation model.

Based on the observed data $S_{j,1}$ for $j = A, B, C$, four conditional likelihood functions are derived as below. Conditional on the realization of the arcing mode evolution process, the conditional likelihood functions given the arcing Joule integrals in all the operation cycles with the AC contactor being in arcing modes I, II, III, and IV are respectively expressed as:

$$\begin{cases} l_2(\boldsymbol{\theta}) = \prod_{m=\mathrm{I}}^{\mathrm{IV}} \left\{ \prod_{l=1}^{k_{\mathrm{I},m}} g_{B,C}\left(x_B\left(t_l^{\mathrm{I},m}\right), x_C\left(t_l^{\mathrm{I},m}\right)\right)\right\} \\ l_3(\boldsymbol{\theta}) = \prod_{m=\mathrm{I}}^{\mathrm{IV}} \left\{ \prod_{l=1}^{k_{\mathrm{II},m}} g_{A,C}\left(x_A\left(t_l^{\mathrm{II},m}\right), x_C\left(t_l^{\mathrm{II},m}\right)\right)\right\} \\ l_4(\boldsymbol{\theta}) = \prod_{m=\mathrm{I}}^{\mathrm{IV}} \left\{ \prod_{l=1}^{k_{\mathrm{III},m}} g_{A,B}\left(x_A\left(t_l^{\mathrm{III},m}\right), x_B\left(t_l^{\mathrm{III},m}\right)\right)\right\} \\ l_5(\boldsymbol{\theta}) = \prod_{m=\mathrm{I}}^{\mathrm{IV}} \left\{ \prod_{l=1}^{k_{\mathrm{IV},m}} g_{A,B,C}\left(x_A\left(t_l^{\mathrm{IV},m}\right), x_B\left(t_l^{\mathrm{IV},m}\right), x_C\left(t_l^{\mathrm{IV},m}\right)\right)\right\} \end{cases} \tag{28}$$

Based on the observed data $S_{j,2}$ for $j = A, B, C$, a conditional likelihood function is derived as below. Conditional on the realization of the arcing mode evolution process, the conditional likelihood function given the arcing Joule integrals in the t_k-th operation cycle is expressed as:

$$\begin{aligned}l_6(\boldsymbol{\theta}) &= h\left(x_A(t_k), x_B(t_k), x_C(t_k)\right) \\ &= \begin{cases} g_{B,C}\left(x_B(t_k), x_C(t_k)\right), & M(t_k) = \mathrm{I} \\ g_{A,C}\left(x_A(t_k), x_C(t_k)\right), & M(t_k) = \mathrm{II} \\ g_{A,B}\left(x_A(t_k), x_B(t_k)\right), & M(t_k) = \mathrm{III} \\ g_{A,B,C}\left(x_A(t_k), x_B(t_k), x_C(t_k)\right), & M(t_k) = \mathrm{IV} \end{cases}\end{aligned} \tag{29}$$

Finally, by combining $l_i(\boldsymbol{\theta})$, $i = 1,2,\ldots,6$, the following complete likelihood function is constructed to update the vector $\widehat{\boldsymbol{\theta}}$ of all the model parameter estimates.

$$L(\boldsymbol{\theta}) = l_1(\boldsymbol{\theta}) l_2(\boldsymbol{\theta}) l_3(\boldsymbol{\theta}) l_4(\boldsymbol{\theta}) l_5(\boldsymbol{\theta}) l_6(\boldsymbol{\theta}) \tag{30}$$

Because of the complexity of $L(\boldsymbol{\theta})$, there is no closed-form estimator of $\boldsymbol{\theta}$. Thus, we formulate an optimization problem as $\max_{\boldsymbol{\theta}} L(\boldsymbol{\theta})$. We solve this optimization problem to determine the estimate of $\boldsymbol{\theta}$ by the genetic algorithm, which has been proven to be an efficient method for solving optimization problems in many studies [31]. Additionally, to ensure the effectiveness and efficiency of parameter estimation, we first obtain rough estimate of $\boldsymbol{\theta}$, which is then used as the initial solution for the genetic algorithm. This rough estimate is obtained through the following method. The rough estimate of $P_{n,m}$ for $n, m = \mathrm{I}, \mathrm{II}, \mathrm{III}$ is determined by calculating the proportion of transitions from arcing mode n to arcing mode m. The rough estimate of ε is set to 1. The rough estimates of $\eta_j, \delta_j, \rho_j, \lambda_j, \phi_j^U, \phi_j^L$ for $j = A, B, C$ are obtained by conducting parameter estimation for each marginal degradation process, with the neglect of the correlation among the arcing Joule integrals of the three-phase contact pairs. Next, the rough estimates of $\rho_{A,B}, \rho_{A,C}, \rho_{B,C}, v$ are determined by two steps. Firstly, for simplification, $\rho_{A,B}, \rho_{A,C}, \rho_{B,C}$ are assumed to be equal for the purpose of calculating the rough estimates. Secondly, by substituting the rough estimates of all the parameters, excluding $\rho_{A,B}, \rho_{A,C}, \rho_{B,C}, v$, into (30), the rough estimates of $\rho_{A,B}, \rho_{A,C}, \rho_{B,C}, v$ are determined though the maximization of (30).

2) Failure Threshold Distributions Updating: Due to the competing failure relationship among the three contact pairs, the failure threshold of the contact pair of phase j must exceed the cumulative arcing Joule integral $y_j(t_k)$ between the contact pair for all $j = A, B, C$, when the AC contactor operates normally up to the current operation cycle t_k. This implies that $D_j | y_j(t_k)$ follows the truncated normal distribution in the interval $\left(y_j(t_k), +\infty\right)$, deviating from the initial distribution $N(\mu_D, \sigma_D^2)$.

Based on the analysis of conditional probability and given the current operation cycle t_k, the updated CDF of the failure threshold is derived by:

$$\begin{aligned} F_{j,t_k}(d) &= Pr\{D_j \le d | y_j(t_k) < D_j < \infty\} \\ &= \frac{Pr\{y_j(t_k) < D_j \le d\}}{Pr\{y_j(t_k) < D_j < \infty\}} \\ &= \frac{\Phi\left(\frac{d-\mu_D}{\sigma_D}\right) - \Phi\left(\frac{y_j(t_k)-\mu_D}{\sigma_D}\right)}{1-\Phi\left(\frac{y_j(t_k)-\mu_D}{\sigma_D}\right)} \end{aligned} \quad (31)$$

where $j = A, B, C$ and $\Phi(\cdot)$ is the CDF of the standard normal distribution. According to (31), the failure threshold distributions of all the three contact pairs can be updated.

4.2. Monte Carlo simulation based RUL prediction

For the contact pair of a phase, failure occurs when the cumulative arcing Joule integral between this contact pair reaches its failure threshold. Moreover, the contact pairs of phases A, B, and C exhibit a competing failure relationship, meaning that the failure of the contact pair of any phase can result in the failure of the AC contactor. Therefore, when the current operation cycle number is t_k, we define the RUL T as:

$$T = \inf\{\tau | \cup_{j=A,B,C}\{Y_j(t_k + \tau) \ge D_j | y_j(t_k)\}\} \quad (32)$$

The expected value of RUL typically serves as the point estimate of RUL [32, 33]. Given the complexity of the proposed model, obtaining the closed-form expression for the RUL expectation is difficult. To address this problem, a Monte Carlo simulation based algorithm, Algorithm 1, is provided to approximate the RUL expectation.

Algorithm 1: Computation of the RUL prediction $\hat{T}$.

Input: The parameters $\boldsymbol{\theta}$ of the proposed three-phase contact pair degradation model, and the parameters $\boldsymbol{\theta}_D$ of the initial distribution of the failure threshold.
Output: The RUL prediction $\hat{T}$.
Initialization: Let p be the number of simulations, and τ_p be the p-th simulated RUL. Let d_j, $x_j(t)$, and $y_j(t)$ be the realizations of D_j, $X_j(t)$, and $Y_j(t)$, respectively.

for p in 1 to N **do**
  Generate d_A, d_B, and d_C from (31) and set $\tau_p = 0$.
  while $y_j(t_k + \tau_p) < d_j$ for $j = A, B, C$ **do**
    $\tau_p = \tau_p + 1$.
    Generate $x_j(t_k + \tau_p)$ from (19) for $j = A, B, C$.
    Set $y_j(t_k + \tau_p) = y_j(t_k + \tau_p - 1) + x_j(t_k + \tau_p)$ for $j = A, B, C$.
  end while
end for
Compute the RUL prediction by $\hat{T} = N^{-1}\sum_{p=1}^{N}\tau_p$.

5. Case study

This section validates the rationality and advantages of the proposed method through a real case and a numerical case. In each case, the RUL of each AC contactor at a current operation cycle is predicted based on degradation data from the corresponding AC contactor. These data consist of the cumulative arcing Joule integrals of the three-phase contact pairs, collected from the first operation cycle up to the current one.

Recent representative state-of-the-art methods for predicting the RUL of an AC contactor include three kinds, namely, the highest degradation level (HDL) method [9], the average degradation level (ADL) method [7], and the model regression (MR) method [8,11]. Moreover, to demonstrate the necessity of accounting for zero and bounded degradation increments, the t copula method is considered [24,30]. Thus, the comparative analysis of these four methods, along with the proposed method, is conducted in each case. The outlines of these methods are as follows.

In the HDL method [9], the degradation data of the contact pair exhibiting the highest degradation level at the current operation cycle are used to reflect the degradation process of an AC contactor. The Wiener process model is adopted to capture this degradation process, followed by predicting the RUL of the AC contactor using a fixed failure threshold. This threshold is prespecified through averaging the failure thresholds of the failed contact pairs in other AC contactors of the same type.

In the ADL method [7], the average degradation level of the three-phase contact pairs is employed to quantify the performance state of an AC contactor. The Wiener process model is applied to model the evolution of the average degradation level, and it is then used to predict the RUL given a fixed failure threshold. The determination process of this threshold is consistent with the HDL method.

In the MR method [8], the unitary regression model is employed to capture the relationship between the degradation levels of the three-phase contact pairs and the RULs of AC contactors. Then, the RUL of an AC contactor is predicted using this model, which is trained based on the degradation data and actual RULs from other AC contactors.

In the t copula method, the cumulative arcing Joule integrals of the three-phase contact pairs are employed to reflect the degradation of an AC contactor. The TEDP model is applied to capture each marginal degradation process [30], and the

correlation among the increments of the three marginal degradation processes is then described using the t copula [24]. The RUL is predicted by considering random failure thresholds, which are modeled and updated in the same way as the proposed method. Notably, the t copula method can be viewed as a simplified version of the proposed model by omitting the consideration of arcing mode transitions.

The average absolute error AE and the average relative error RE are employed to compare the prediction accuracy of the five methods. The relative superiority index [34] is used to measure the difference among different methods. Let ARE_i for i=1,2,3,4,5 denote the average absolute or relative error for the i-th method. Then, the relative superiority index of the i-th method is expressed as:

$$RS_i = \frac{ARE_i}{\min\limits_{1\le j\le 5}\{ARE_j\}} \tag{33}$$

Moreover, in the case study, the total number of simulations N in Algorithm 1 is set to 8,000. This value is determined by analyzing the convergence behavior of the predicted RUL with respect to N using degradation data from the real case. The predicted RUL stabilizes when N reaches approximately 8,000, meaning that further increasing N leads to negligible changes. Specifically, the difference between the predicted RULs at $N = 8{,}000$ and $N = 8{,}001$ is less than 20 cycles, which is far smaller than the lifespans of AC contactors. Therefore, $N = 8{,}000$ is adopted.

5.1. Real case

The rationality for considering multiple arcing modes and competing failure in the proposed method is demonstrated in Subsection 5.1-1. The superiority of the proposed method is then presented in Subsection 5.1-2. The real degradation data of cumulative arcing Joule integrals used in Subsections 5.1-1 and 5.1-2 were obtained from three CJX2-32 AC contactors during the AC-4 electrical life test, the configuration of which is shown in Table 1 [9]. The AC contactors were tested under the AC-4 condition, which aligns with the operation condition of AC contactors widely used in common assembly lines. This configuration is implemented for AC contactors to control motors for standard functions, including starting, braking, and reversing operations [26].

Table 1. Configuration of the AC-4 electrical life test.

Parameter	Configuration
Rated voltage	380 V
Rated current	32 A
Test voltage	380 V
Test current	192 A
Power factor	0.65
Electricity frequency	50 Hz
Voltage on the coil	380 V

1) Rationality Analysis of the Proposed Model: Fig. 3 presents the degradation data of the cumulative arcing Joule integrals over the entire lifespans of the three CJX2-32 AC contactors (labeled as Contactor #1 to Contactor #3). The test result showed that, for Contactor #1, the waveform of the current carried by the contact pair of phase B ultimately demonstrated instability, signifying poor connectivity and failure of this contact pair, which caused the failure of Contactor #1. It was also observed that the contact pairs of phase A were failed for Contactor #2 and Contactor #3. Moreover, Fig. 3 illustrates that the cumulative arcing Joule integral of the failed contact pair is higher than those of the two non-failed contact pairs at the end of the lifespan of each AC contactor. This implies that the contact pair ultimately suffering the most severe accumulative electrical erosion among the three contact pairs is the failed one. Additionally, for each AC contactor, the cumulative arcing Joule integrals of the three-phase contact pairs lead alternately during operation. This suggests that the degrees of the accumulative electrical erosions of the three contact pairs may lead alternately, owing to the randomness in the accumulation process of electrical erosion. This phenomenon creates difficulty in determining which pair of contacts will ultimately fail when an AC contactor does not fail. Therefore, it is rational to account for the competing failure relationship among the three-phase contact pairs in the proposed method.

Fig. 4 illustrates the arcing mode in each operation cycle for Contactors #1 to #3. Meanwhile, based on the degradation data of Contactors #1 to #3, the statistical result of the percentage of operation cycles in which no arcing occurs between a contact pair (that is, the AC contactor is in arcing mode I, II, or III) relative to the entire lifespan is 5.3956%. This result shows that an AC contactor operates in arcing mode I, II, or III within many operation cycles. In other words, the phenomenon of zero arcing

Joule integrals (i.e., zero degradation increments) between a contact pair occurs in many operation cycles. Thus, considering zero degradation increments in the proposed method is rational.

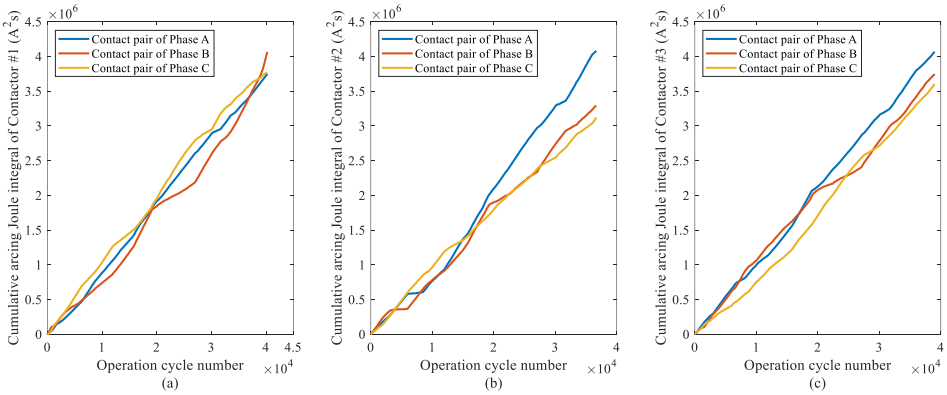

Figure 3. (a) Cumulative arcing Joule integrals of Contactor #1, (b) cumulative arcing Joule integrals of Contactor #2, and (c) cumulative arcing Joule integrals of Contactor #3.

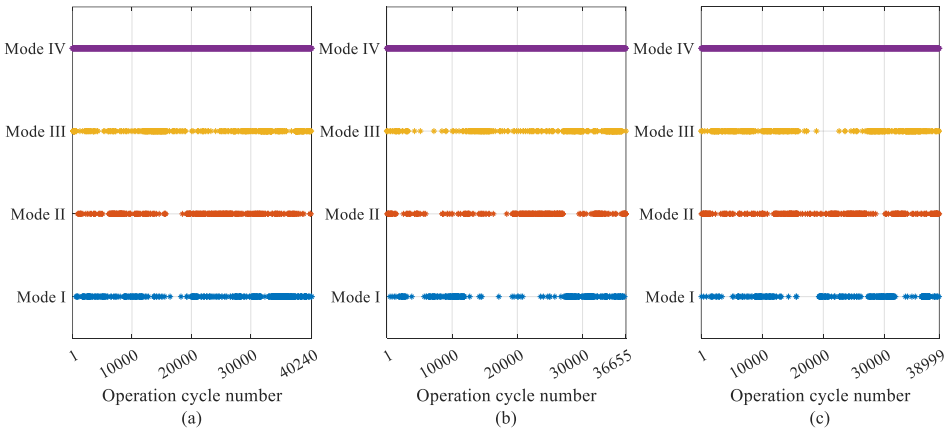

Figure 4. (a) Arcing modes of Contactor #1, (b) arcing modes of Contactor #2, and (c) arcing modes of Contactor #3.

Table 2. Minimum and maximum arcing joule integral values.

	Phase	Contactor #1	Contactor #2	Contactor #3
Experimental result	Phase A	[9.7000, 263.7300]	[9.5700, 271.7700]	[10.2600, 260.3700]
	Phase B	[8.8600, 276.5100]	[8.3800, 259.2000]	[9.6800, 256.8500]
	Phase C	[7.8200, 274.8100]	[10.5800, 262.6400]	[7.9200, 263.7800]
Estimated theoretical result	Phase A	[5.6312, 279.2341]	[7.9771, 275.9890]	[6.3752, 273.6860]
	Phase B	[8.2572, 286.4671]	[8.3465, 292.3729]	[8.9334, 282.2393]
	Phase C	[4.7412, 283.0681]	[6.9515, 279.2758]	[4.2453, 280.2048]

Table 2 presents the minimum and maximum values of the arcing Joule integrals, based on the degradation data from the entire lifespans of Contactors #1 to #3. Firstly, the minimum and maximum values are recorded from the degradation data of Contactors #1 to #3, as shown in the row labeled "Experimental result" in Table 2. Since the minimum value is clearly larger than zero and the maximum value is not excessively high, the experimental result supports that the arcing Joule integral has both lower and upper bounds. Secondly, the minimum and maximum values are estimated using (30), as shown in the row labeled "Estimated theoretical result" in Table 2. Given the supportive experimental and reasonable estimated theoretical results, considering bounded degradation increments in the proposed method is rational.

Table 3. Critical breaking phase angles.

	Phase	Contactor #1	Contactor #2	Contactor #3
Experimental result	Phase A	[0.1006, 3.0307]	[0.0851, 3.0324]	[0.1020, 3.0271]
	Phase B	[0.0790, 3.0361]	[0.1133, 3.0433]	[0.1286, 3.0312]
	Phase C	[0.0851, 3.0586]	[0.1014, 3.0248]	[0.0856, 3.0441]
Estimated theoretical result	Phase A	[0.0682, 3.0839]	[0.0686, 3.0719]	[0.0699, 3.0813]
	Phase B	[0.0517, 3.0679]	[0.0490, 3.0670]	[0.0615, 3.0407]
	Phase C	[0.0584, 3.0963]	[0.0680, 3.0797]	[0.0668, 3.1113]

Table 3 shows the critical breaking phase angles ϕ_j^L and ϕ_j^U for phase $j, j = A, B, C$, based on the degradation data from the entire lifespans of Contactors #1 to #3. Here, ϕ_j^L and ϕ_j^U are the lower and upper bounds of the arcing phase angle, which is the breaking phase angle with which an arc can be generated. As exhibited in the row labeled "Experimental result" in Table 3, the experimental values of ϕ_j^L and ϕ_j^U are calculated by (7) based on the degradation data from Contactors #1 to #3. Since the experimental lower and upper bounds are not much close to 0 and π, respectively, the result supports the existence of the critical breaking phase angles. Then, the theoretical values of ϕ_j^L and ϕ_j^U are estimated using (30), as exhibited in the row labeled "Estimated theoretical result" in Table 3. Due to the supportive experimental result and the reasonable estimated theoretical result, it is rational to introduce the critical breaking phase angles.

Based on the degradation data from the entire lifespans of Contactors #1 to #3, the Kendall rank correlation coefficients are calculated as $\gamma_{A,B} = -0.4953$, $\gamma_{A,C} = -0.5132$, and $\gamma_{B,C} = -0.5079$. The coefficient $\gamma_{k,l}$ measures the nonlinear correlation between the arcing Joule integrals of phases k and l. The Kendall rank correlation coefficient is a widely used metric for assessing nonlinear correlation in statistical analysis, with its computational formula given by [18]:

$$\gamma_{k,l} = \frac{2}{\pi}\arcsin(\rho_{k,l}) \tag{34}$$

where $\rho_{k,l}$ is the correlation coefficient in (22). The calculated Kendall rank correlation coefficients, all approximately -0.5, confirm the nonlinear correlation between the arcing Joule integrals of any two phases in which arcing occur. Statistically, a Kendall coefficient of -0.5 corresponds to a probability of 0.75 that the arcing Joule integrals of two phases will move in opposite directions [35]. Hence, neglecting this correlation would discard valuable degradation information and lead to an inaccurate description of the degradation processes of AC contactors. Thus, it is essential to consider nonlinear degradation correlation.

In conclusion, the rationality for considering multiple arcing modes and competing failure, along with the introduction of the critical breaking phase angles, has been validated. Here, the characteristic of multiple arcing modes is represented in three aspects, including zero degradation increments, bounded degradation increments, and nonlinear degradation correlation.

2) Prediction Accuracy Analysis of the Proposed Method: To validate the advantages of the proposed method, we apply the five methods mentioned at the beginning of Section 5 to predict the RULs of Contactors #1 to #3 over multiple current operation cycles, using the degradation data shown in Fig. 3. When predicting the RUL of an AC contactor, it is assumed that the degradation data from the other two AC contactors are known, which allows for the determination of the initial failure threshold distribution, as detailed in Subsection 3.4. Figs. 5 to 7 display the RUL predictions for Contactors #1 to #3 and their corresponding prediction errors. Tables 4 to 6 present the average prediction errors for Contactors #1 to #3 and their corresponding relative superiority indices.

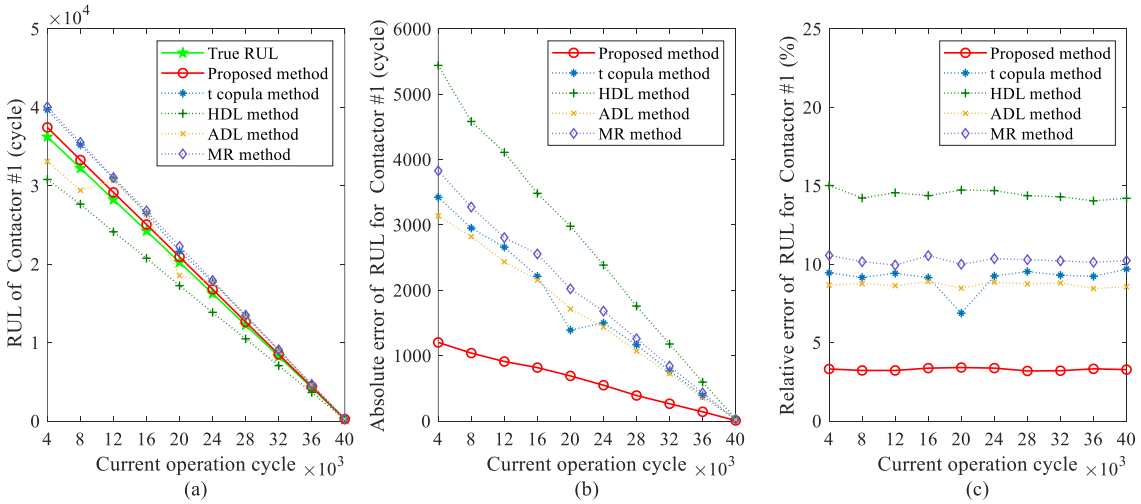

Figure 5. (a) RUL predictions, (b) absolute errors, and (c) relative errors for Contactor #1.

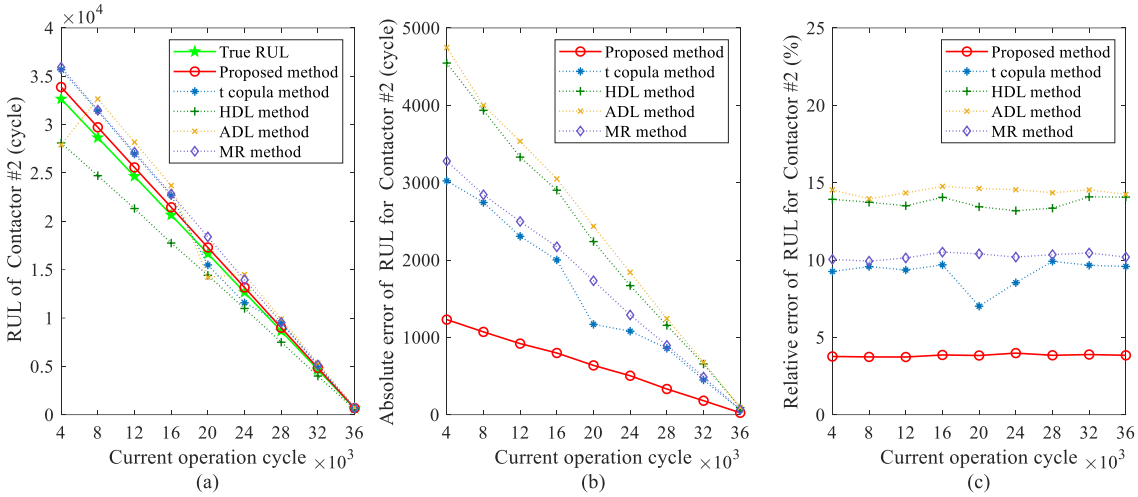

Figure 6. (a) RUL predictions, (b) absolute errors, and (c) relative errors for Contactor #2.

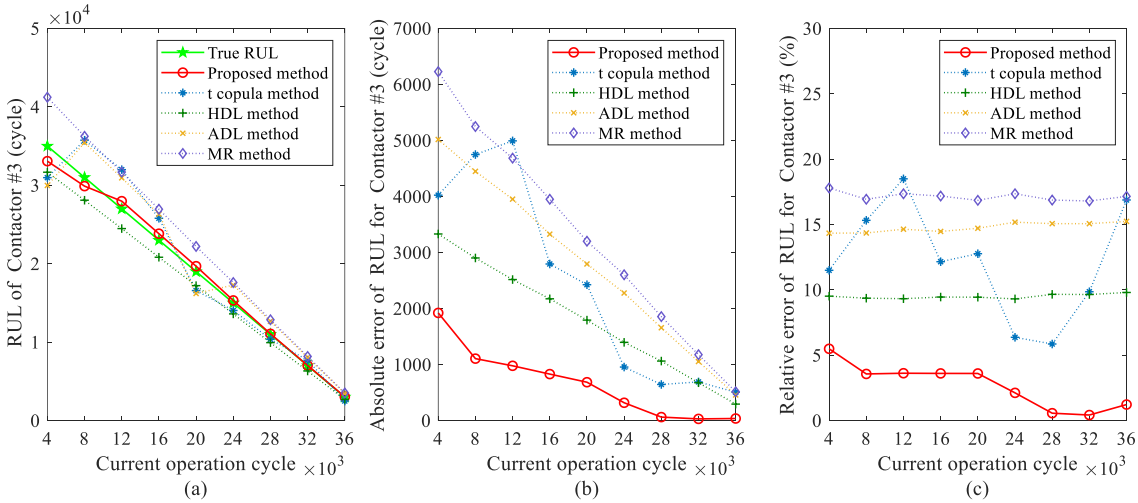

Figure 7. (a) RUL predictions, (b) absolute errors, and (c) relative errors for Contactor #3.

Table 4. Average errors and their corresponding relative superiority indices for Contactor #1.

	Average error		Relative superiority	
Error	$AE(10^3)$	$RE(\%)$	AE	RE
Proposed	0.6012	3.2924	1.0000	1.0000
t copula method	1.6490	9.1008	2.7430	2.7642
HDL method	2.6552	14.4481	4.4168	4.3883
ADL method	1.5880	8.6812	2.6416	2.6367
MR method	1.8725	10.2402	3.1148	3.1102

Table 5. Average errors and their corresponding relative superiority indices for Contactor #2.

	Average error		Relative superiority	
Error	$AE(10^3)$	$RE(\%)$	AE	RE
Proposed	0.6330	3.8304	1.0000	1.0000
t copula method	1.5214	9.1749	2.4033	2.3953
HDL method	2.2803	13.7034	3.6021	3.5776
ADL method	2.4017	14.4301	3.7939	3.7673
MR method	1.6956	10.2417	2.6785	2.6738

Table 6. Average errors and their corresponding relative superiority indices for Contactor #3.

	Average error		Relative superiority	
Error	$AE(10^3)$	$RE(\%)$	AE	RE
Proposed	0.6629	2.6916	1.0000	1.0000
t copula method	2.4202	12.1321	3.6509	4.5075
HDL method	1.7939	9.5007	2.7061	3.5298
ADL method	2.7764	14.7842	4.1882	5.4928
MR method	3.2736	17.1423	4.9383	6.3689

For illustration, consider Contactor #1 as an example. Fig. 5 demonstrates that for Contactor #1, the relative errors of the proposed method do not exhibit a clear variation trend, which may be because the true RULs also decrease over the current operation cycle. It is also observed from Fig. 5 that the absolute errors of the proposed method generally decrease as the current operation cycle progresses. This phenomenon is explained as follows. As the size of degradation data increases, the degradation characteristics, such as competing failure and multiple arcing modes, may gradually sufficiently emerge, and

the corresponding statistical laws may tend to be stable. Then, the estimates of the model parameters may tend to converge, which is supported by the estimation result in Fig. 8. Here, Fig. 8 shows the evolution of the estimates for the model parameters ϕ_j^L and ϕ_j^U (i.e., the lower and upper bounds of the arcing phase angle) for $j = A, B, C$. Since the proposed model contains many parameters and the others exhibit similar convergence trends, their estimates at the current operation cycle of 40,000 are shown in Table 7. Additionally, the model parameters are estimated using the method described at the end of Subsection 4.1-1. Since the estimates tend to converge with the increase of data as shown in Fig. 8, it can be deduced that the proposed estimation method can ensure stable estimates, which indicates its effectiveness. Furthermore, owing to the increasingly stable statistical laws of the degradation characteristics and the gradually convergent estimates of the model parameters, the discrepancy between the obtained degradation model and the real degradation process may reduce. This further leads to the decrease of the absolute error. As shown in Figs. 6 and 7, similar variation laws of the errors can be observed for Contactor #2 and Contactor #3.

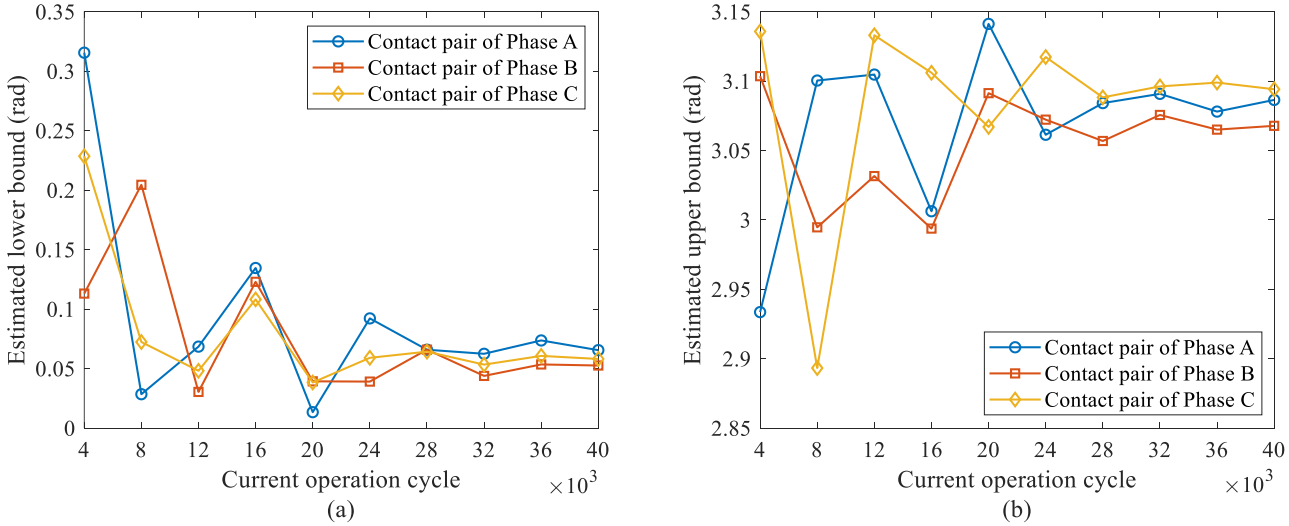

Figure 8. (a) Estimated lower bound and (b) upper bound of the arcing phase angle.

Table 7. Parameter estimates of the proposed model.

Parameter	Estimate
$(P_{\mathrm{I,I}}, P_{\mathrm{I,II}}, P_{\mathrm{I,III}}, P_{\mathrm{II,I}}, P_{\mathrm{II,II}})'$	$(0.0407, 0.012, 0.0060, 0.0222, 0.0202)'$
$(P_{\mathrm{II,III}}, P_{\mathrm{III,I}}, P_{\mathrm{III,II}}, P_{\mathrm{III,III}}, \varepsilon)'$	$(0.0242, 0.0072, 0.0058, 0.0420, 1.6461)'$
$(\eta_A, \delta_A, \rho_A, \lambda_A)'$	$(71.8580, 1.0245, 1.3450, 0.0679)'$
$(\eta_B, \delta_B, \rho_B, \lambda_B)'$	$(17.6324, 1.1647, 1.6242, 0.0478)'$
$(\eta_C, \delta_C, \rho_C, \lambda_C)'$	$(126.4956, 0.9718, 1.5063, 0.1752)'$
$(\rho_{A,B}, \rho_{A,C}, \rho_{B,C}, v)'$	$(-0.6961, -0.7439, -0.7199, 56.7096)'$

Fig. 5 and Table 4 show that for Contactor #1, the proposed method consistently exhibits the smallest prediction errors at all the current operation cycles. This indicates that the proposed method consistently outperforms the other methods in terms of the prediction accuracy across all the current operation cycles. Additionally, according to the prediction results for Contactors #2 and #3 presented in Figs. 6 and 7, as well as Tables 5 and 6, a similar outcome can be observed, showing that the proposed method outperforms the other methods in terms of the prediction accuracy.

Subsection 5.1-1 illustrates that the degradation of AC contactors is characterized by competing failure and multiple arcing modes. Here, the characteristic of multiple arcing modes is represented by zero degradation increments, bounded degradation increments, and nonlinear degradation correlation. Although the t copula method accounts for competing failure and nonlinear degradation correlation, it fails to consider zero and bounded degradation increments because each marginal

degradation process is captured by the TEDP model. In contrast, the proposed method captures zero and bounded degradation increments through the modeling of arcing mode transitions. Thus, the superior prediction accuracy of the proposed method over the t copula method demonstrates that incorporating arcing mode transitions effectively improves RUL prediction performance.

For the HDL and ADL methods, they treat the three-phase contact pairs as a whole, failing to separately describe the degradation process of each individual contact pair. In other words, these methods depict the degradation of an AC contactor as a single degradation process, overlooking the effects of competing failure and multiple arcing modes. This potentially leads to an inaccurate description of the degradation of AC contactors. Moreover, both the HDL and ADL methods use a fixed prespecified failure threshold, neglecting its randomness. To explain the reason that the failure threshold cannot be considered as a fixed value, the parameters in the failure threshold distribution are estimated using the method given in Appendix-A, based on the degradation data from the entire lifespans of Contactors #1 to #3. The estimate is:

$$\widehat{\boldsymbol{\theta}}_D = (\hat{\mu}_D, \hat{\sigma}_D^2)' = (4.0723 \times 10^6,\ 6.8766 \times 10^7)' \quad (35)$$

which suggests the significant randomness of the failure threshold due to the considerably large variance $\hat{\sigma}_D^2 = 6.8766 \times 10^7$. Therefore, resulting from the inaccurate description of the degradation characteristics and the neglect of the randomness of the failure threshold, these methods cannot ensure a high accuracy of RUL prediction.

The MR method depends on prior data from other AC contactors. Nevertheless, there may be differences between the AC contactor whose RUL needs to be predicted and the ones providing the prior data. These differences could stem from factors such as inherent unit-to-unit variations, potentially reducing the accuracy of RUL prediction. Such differences can be reflected by the degradation processes and failure thresholds of different AC contactors. Firstly, it can be observed from Fig. 3 that different contact pairs of different AC contactors have distinct degradation processes. According to the proposed degradation model, the overall degradation trend of the contact pair for phase $j, j = A, B, C$ is described by $\eta_j t^{\delta_j}$. Table 8 displays the estimated overall degradation trend of each contact pair in each AC contactor, based on all the degradation data shown in Fig. 3. From Table 8, the overall degradation trends of the contact pairs of phase A are estimated as $\hat{\eta}_A t^{\hat{\delta}_A} = 71.8580t^{1.0245}$, $\hat{\eta}_A t^{\hat{\delta}_A} = 33.1908t^{1.1152}$, and $\hat{\eta}_A t^{\hat{\delta}_A} = 90.6669t^{1.0133}$ for Contactors #1 to #3, respectively. Although the estimates of δ_A for Contactors #1 to #3 are close, the estimate of η_A for Contactor #3 is 26.1751% higher and 173.1690% higher than those for Contactors #1 and #2, respectively. This indicates that the overall degradation trend for the contact pair of phase A differs across different AC contactors. Similarly, the overall degradation trends for the contact pairs of phases B and C also show variations across different AC contactors. Additionally, the large variance $\hat{\sigma}_D^2 = 6.8766 \times 10^7$ of the failure threshold also demonstrates the differences among different AC contactors. Therefore, resulting from the differences reflected by the degradation processes and the failure thresholds, the MR method may be unable to achieve a reliable RUL prediction performance.

Table 8. Estimated overall degradation trend of each contact pair in each AC Contactor.

	Contactor #1	Contactor #2	Contactor #3
Phase A ($\hat{\eta}_A t^{\hat{\delta}_A}$)	$71.8580t^{1.0245}$	$33.1908t^{1.1152}$	$90.6669t^{1.0133}$
Phase B ($\hat{\eta}_B t^{\hat{\delta}_B}$)	$17.6324t^{1.1647}$	$72.2293t^{1.0208}$	$104.3593t^{0.9922}$
Phase C ($\hat{\eta}_c t^{\hat{\delta}_c}$)	$126.4956t^{0.9718}$	$125.0924t^{0.9634}$	$44.6363t^{1.0688}$

The proposed method presents several advantages over the other methods. In terms of degradation modeling, it comprehensively considers competing failure and multiple arcing modes. Specifically, the transition among the arcing modes is captured by the proposed arcing mode evolution model, which is constructed by measuring the similarity between the actual and imaginary arcing Joule integrals of the three-phase contact pairs. Both zero and bounded degradation increments are captured by the proposed doubly truncated TEDP model with zero increments, derived from the analysis of the arcing mechanism. Nonlinear degradation correlation is captured by the t copula. In terms of RUL prediction, an analytical likelihood function is derived, based on which the model parameters are updated as degradation data accumulates. The truncated normal distribution is used to model the randomness of the failure threshold, and it is updated using conditional probability analysis as the size of degradation data increases.

Moreover, the proposed method updates the model parameters without the degradation data from other AC contactors. Therefore, the proposed method can achieve superior prediction accuracy compared to the other methods.

Fig. 9(a) presents boxplots of the absolute errors of the RUL predictions for all methods, based on the entire lifespan degradation data of Contactors #1 to #3. As shown, the proposed method achieves the lowest median and the narrowest interquartile range, indicating both high accuracy and stable prediction performance. Fig. 9(b) presents boxplots based on the first third of the degradation data of Contactors #1 to #3, which are relatively small compared to the entire lifespan degradation data. In this small-sample condition, the proposed method again exhibits the lowest median and the narrowest interquartile range. This indicates that even under the small-sample condition, where parameter estimates may not yet be stable, the proposed method still maintains the highest prediction accuracy, demonstrating its effectiveness in mitigating overfitting risk. This advantage stems from the fact that the degradation model is constructed based on arcing mechanism analysis and the degradation characteristics of AC contactors, rather than relying solely on data fitting.

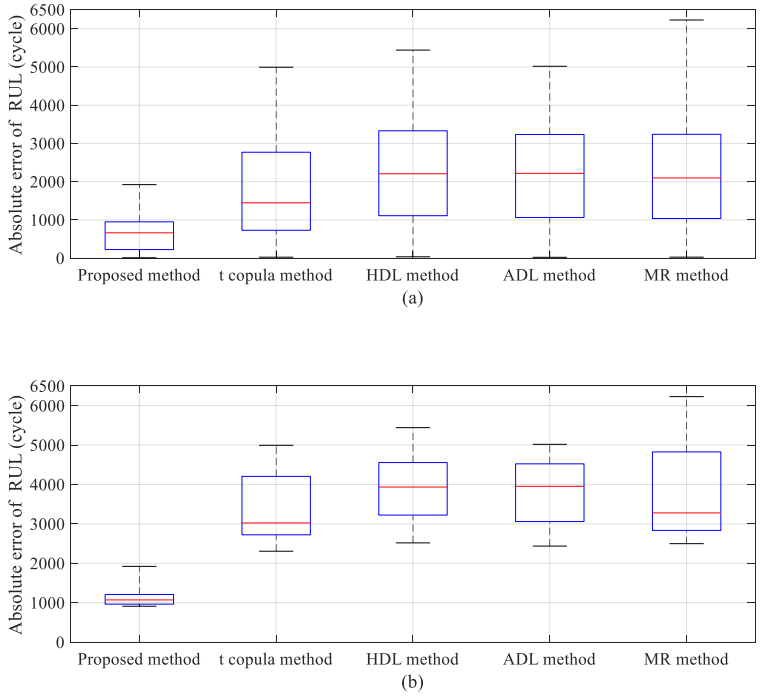

Figure 9. Boxplots of absolute errors for Contactors #1 to #3 based on (a) the entire lifespan degradation data and (b) the first third of the degradation data.

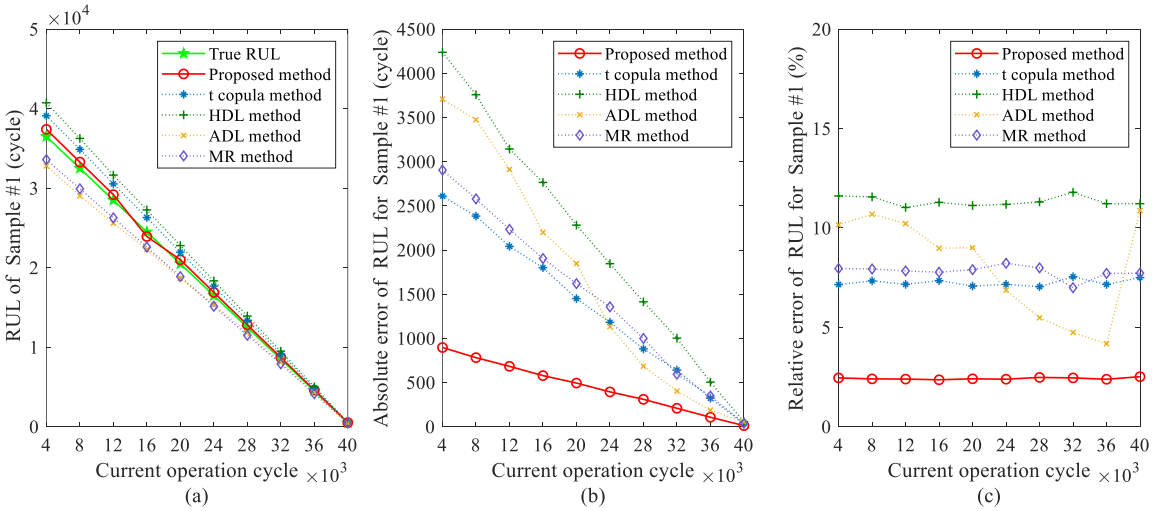

Figure 10. (a) RUL predictions, (b) absolute errors, and (c) relative errors for Sample #1.

5.2. Numerical case

A numerical case is provided to further demonstrate the advantages of the proposed method over the other methods. Using the Monte Carlo simulation algorithm detailed in Appendix-B, we generate the degradation data of 1,000 AC contactors, labeled as Samples #1 to #1,000.

For illustration, the degradation data of Sample #1 are used to display the prediction performances of the five methods. Fig. 9 shows the RUL predictions of Sample #1 and their corresponding prediction errors. Table 9 displays the average prediction errors of Sample #1 and their corresponding relative superiority indices.

Table 9. Average errors and their corresponding relative superiority indices for sample #1.

	Average error		Relative superiority	
Error	$AE(10^3)$	$RE(\%)$	AE	RE
Proposed	0.4469	2.4265	1.0000	1.0000
t copula method	1.3351	7.2487	2.9878	2.9873
HDL method	2.1009	11.3344	4.7015	4.6710
ADL method	1.6604	8.1188	3.7158	3.3458
MR method	1.4578	7.8053	3.2624	3.2166

Fig. 9 illustrates that for Sample #1, the absolute errors across all the methods generally decrease as the current operation cycle progresses, and the relative errors do not exhibit a clear trend. Fig. 9 and Table 9 show that for Sample #1, the proposed method consistently exhibits the smallest prediction errors at all the current operation cycles. This indicates that the proposed method consistently outperforms the other methods in terms of the prediction accuracy across all the current operation cycles.

Both the HDL and ADL methods neglect the influences of competing failure and multiple arcing modes. The MR method fails to address the distinction between the degradation process of the AC contactor whose RUL needs to be predicted and the degradation processes of the ones supplying the prior data. The t copula method does not consider zero and bounded degradation increments. In contrast, the proposed method constructs the models that fully capture the degradation characteristics of AC contactors. Simultaneously, it updates the models using only the degradation data from the AC contactor whose RUL needs to be predicted, without degradation data from other AC contactors.

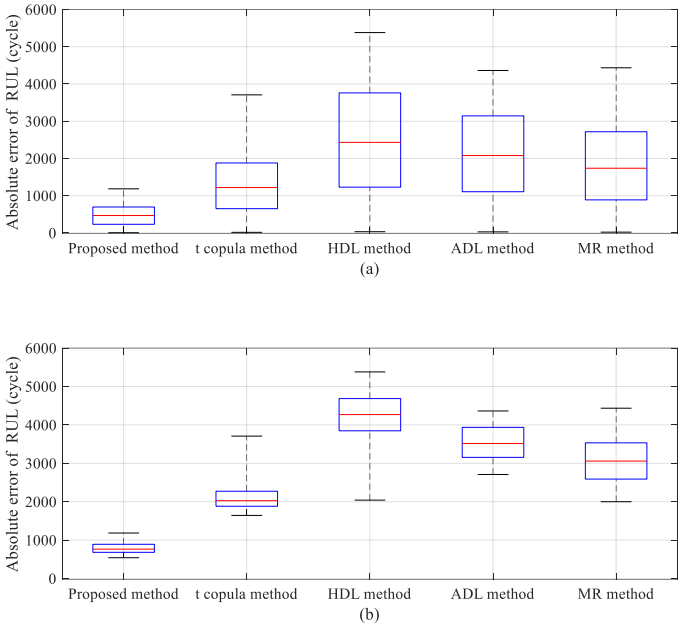

Figure 11. Boxplots of absolute errors for all simulated samples based on (a) the entire lifespan degradation data and (b) the first third of the degradation data.

Fig. 11 presents boxplots of the absolute errors of the RUL predictions for all methods, with Fig. 11(a) based on the entire lifespan degradation data of all simulated samples and Fig. 11(b) based on the first third of the degradation data. In Fig. 11(a), the proposed method exhibits the lowest median and the narrowest interquartile range, demonstrating superior and stable prediction accuracy. Fig. 11(b) shows similar patterns under small-sample conditions, reflecting the effectiveness of the proposed method in mitigating overfitting risk.

6. Conclusion

In this paper, a RUL prediction method was proposed for AC contactors based on a novel Doubly Truncated Degradation Model Considering Arcing Mode Transitions. Specifically, the physical model of the arcing Joule integral was derived, based on which the characteristics of zero and bounded degradation increments were theoretically validated, and four arcing modes were identified. The degradation process was properly modeled by comprehensively considering competing failure and multiple arcing modes. Then, a Monte Carlo simulation based RUL prediction algorithm that incorporates model updating was provided. Through the real case, it was illustrated that the degradation of AC contactors is characterized by competing failure, as well as multiple arcing modes represented by zero degradation increments, bounded degradation increments, and

nonlinear degradation correlation. Furthermore, both the real and numerical cases demonstrated that the proposed method can achieve a favorable accuracy of RUL prediction.

In the proposed method, RUL is approximated using Monte Carlo simulation. To improve computational efficiency, a more efficient sampling method, such as the Metropolis-Hastings algorithm, can be employed in a future work. Moreover, predictive maintenance strategies for AC contactors and production planning considering the reliability of AC contactors can be investigated based on the proposed RUL prediction method. Additionally, the proposed degradation model can be extended for other products that have characteristics such as mode transition and bounded degradation increments.

Acknowledgements

This work was supported in part by the Continuation Funding Project for Innovative Research Groups of Natural Science Foundation of Hebei Province under Grant E2024202298, in part by the National Natural Science Foundation of China under Grant 51937004, in part by the S&T Program of Hebei under Grant 24464401D, and in part by the National Natural Science Foundation of China under Grant 72101081.

References

1. Xing C, Liu S, Peng S, Gao S, Liu Y, Li J, Cao Y. Remaining electrical life prediction of AC contactor based on CAE-BiGRU-Attention. Measurement Science and Technology 2024; 35(1): 015041, 10.1088/1361-6501/ad05a1.
2. Sun S, Liu J, Wang J, Shao X, Zhao Y. Research on evaluation and prediction method of electrical life of contactor individual. IEEJ Transactions on Electrical and Electronic Engineering 2024; 19(10): 1596–1609. https://doi.org/10.1002/tee.24119.
3. Liu S, Li Y, Peng S, Cao Y. Classification and prediction of AC contactor degradation states based on K-Means clustering and Bayes-BiLSTM. Journal of Electrical Engineering & Technology 2025; 20(3): 1899–1910. 10.1007/s42835-024-02065-6.
4. Xing C, Liu S, Li Y, Xu J, Li J. Degradation stage division and identification of AC contactor's contact system. IEEE Sensors Journal 2025; 25(4): 7068–7078. 10.1109/JSEN.2025.3527471.
5. Tang S, Wang F, Sun X, Xu X, Yu C, Si X. Unbiased parameters estimation and mis-specification analysis of Wiener process-based degradation model with random effects. Applied Mathematical Modelling 2022; 109: 134–160. https://doi.org/10.1016/j.apm.2022.03.039.
6. Cao X, Shi X, Zhao J, Duan Y, Yang X. Dynamic grouping maintenance optimization by considering the probabilistic remaining useful life prediction of multiple equipment. Eksploatacja i Niezawodnosc – Maintenance and Reliability 2024; 26(3): 187793. https://doi.org/10.17531/ein/187793.
7. Li K, Zhao C, Niu F, Zheng S, Duan Y, Huang S, Wu Y. Electrical performance degradation model and residual electrical life prediction for AC contactor. IEEE Transactions on Components, Packaging and Manufacturing Technology 2020; 10(3): 400–417. 10.1109/TCPMT.2020.2966516.
8. Sun S, Wang Q, Du T, Wang J, Li S, Zong J. Quantitative evaluation of electrical life of AC contactor based on initial characteristic parameters. IEEE Transactions on Instrumentation and Measurement 2021; 70: 1–10. 10.1109/TIM.2020.3031160.
9. Zheng S, Niu F, Li K, Huang S, Liu Z, Wu Y. Analysis of electrical life distribution characteristics of AC contactor based on performance degradation. IEEE Transactions on Components, Packaging and Manufacturing Technology 2018; 8(9): 1604–1613. 10.1109/TCPMT.2018.2841425.
10. Ge F, Qiu T, Zhang M, Ji J. Experimental research on the thermal characteristic of low-voltage alternating current (AC) arc faults. Fire Safety Journal 2023; 136: 103732. https://doi.org/10.1016/j.firesaf.2022.103732.
11. Wu Z, Wu G, Huang H, You Y. A novel residual electrical endurance prediction method for low-voltage electromagnetic alternating current contactors. IEEE Transactions on Components, Packaging and Manufacturing Technology 2015; 5(4): 465–473. 10.1109/TCPMT.2015.2415852.
12. Fan W, Gao X, Han L, Xu Z, Chen C, Chen L. Adaptive Multistage Sparse Gaussian Process Regression for Bearing Remaining Useful Life Prediction. IEEE Transactions on Instrumentation and Measurement 2025; 74: 1–10. 10.1109/TIM.2025.3627353.
13. Liu Z, Li Q, Chen X, Ren Y, Cheng Y. Adaptive Remaining Useful Life Prediction Model for Lithium-Ion Batteries Based on Polynomial Fitting. IEEE Transactions on Instrumentation and Measurement 2025; 74: 1–11. 10.1109/TIM.2025.3541667.
14. Deng M, Xu M, Bian W, Liu D, Deng A. Deep Bayesian Stochastic Process Model for Remaining Useful Life Prediction of Rolling Bearings. IEEE Transactions on Instrumentation and Measurement 2025; 74: 1–15. 10.1109/TIM.2025.3635312.

15. Fan L, Xu X, Ni Y. Multi-failure mode reliability of monorail vehicle gear transmission system based on multi-index staged degradation. Applied Mathematical Modelling 2024; 136: 115602, https://doi.org/10.1016/j.apm.2024.07.009.
16. Fang G, Pan R. A class of hierarchical multivariate Wiener processes for modeling dependent degradation data. Technometrics 2024; 66(2): 141–156, https://doi.org/10.1080/00401706.2023.2242413.
17. Yan B, Wang H, Ma X. Correlation-driven multivariate degradation modeling and RUL prediction based on Wiener process model. Quality and Reliability Engineering International 2023; 39(8): 3203–3229. https://doi.org/10.1002/qre.3105.
18. Frahm G, Junker M, Szimayer A. Elliptical copulas: applicability and limitations. Statistics & Probability Letters 2003; 63(3): 275–286. https://doi.org/10.1016/S0167-7152(03)00092-0.
19. Zheng Y, Zhang Y. Reliability analysis for system with dependent components based on survival signature and copula theory. Reliability Engineering & System Safety 2023; 238: 109402. https://doi.org/10.1016/j.ress.2023.109402.
20. Tang X, Li D, Zhou C, Phoon K, Zhang L. Impact of copulas for modeling bivariate distributions on system reliability. Structural Safety 2013; 44: 80–90. https://doi.org/10.1016/j.strusafe.2013.06.004.
21. Sun F, Fu F, Liao H, Xu D. Analysis of multivariate dependent accelerated degradation data using a random-effect general Wiener process and D-vine Copula. Reliability Engineering & System Safety 2020; 204: 107168. https://doi.org/10.1016/j.ress.2020.107168.
22. Zhang J, Yan R, Wang J. Reliability optimization of parallel-series and series-parallel systems with statistically dependent components. Applied Mathematical Modelling 2022; 102: 618–639. https://doi.org/10.1016/j.apm.2021.10.003.
23. Luo X, Shevchenko PV. The t copula with multiple parameters of degrees of freedom: bivariate characteristics and application to risk management. Quantitative Finance 2010; 10(9): 1039–1054, 10.1080/14697680903085544.
24. Demarta S, McNeil A J. The t copula and related copulas. International statistical review 2005; 73(1): 111–129. https://doi.org/10.1111/j.1751-5823.2005.tb00254.x.
25. Ge Q, Menendez M. Exploring the variance contributions of correlated model parameters: A sampling-based approach and its application in traffic simulation models. Applied Mathematical Modelling 2021; 97: 438–462. https://doi.org/10.1016/j.apm.2021.04.012.
26. Shea J J. Modeling contact erosion in three phase vacuum contactors. IEEE Transactions on Components, Packaging and Manufacturing Technology 1998; 21(4): 556–564, 10.1109/95.740048.
27. Luo J, Shao H, Lin J, Liu B. Meta-learning with elastic prototypical network for fault transfer diagnosis of bearings under unstable speeds. Reliability Engineering & System Safety 2024; 245: 110001. https://doi.org/10.1016/j.ress.2024.110001.
28. Chen Z, Xia T, Li Y, Pan E. Random-effect models for degradation analysis based on nonlinear Tweedie exponential-dispersion processes. IEEE Transactions on Reliability 2022; 71(1): 47–62. 10.1109/TR.2021.3107050.
29. Chen Z, Xia T, Li Y, Pan E. Tweedie exponential dispersion processes for degradation modeling, prognostic, and accelerated degradation test planning. IEEE Transactions on Reliability 2020; 69(3): 887–902. 10.1109/TR.2019.2955596.
30. Yan W, Xu X, Bigaud D, Cao W. Optimal design of step-stress accelerated degradation tests based on the Tweedie exponential dispersion process. Reliability Engineering & System Safety 2023; 230: 108917. https://doi.org/10.1016/j.ress.2022.108917.
31. Levitin G, Xing L, Xiang Y. Optimal multiple replacement and maintenance scheduling in two-unit systems. Reliability Engineering & System Safety 2021; 213: 107803. https://doi.org/10.1016/j.ress.2021.107803.
32. Shi R, Lü Y, Zhang Y, Meng J, Chen R, Hu R. Remaining Useful Life Estimation with Coupling Dual Random Effects Based on Nonlinear Wiener Process. Eksploatacja i Niezawodnosc – Maintenance and Reliability 2025; 27(4): 202908. https://doi.org/10.17531/ein/202908.
33. Peng C, Li J, Ren L, Li D, Chen J. Remaining useful life prediction of binary stochastic degradation equipment based on mixed Copula functions. Eksploatacja i Niezawodnosc – Maintenance and Reliability 2026; 28(1): 209903. https://doi.org/10.17531/ein/209903.
34. Li X, Chen D, Wu J, Kang R. 3-Dimensional general ADT modeling and analysis: Considering epistemic uncertainties in unit, time and stress dimension. Reliability Engineering & System Safety 2022; 225: 108577. https://doi.org/10.1016/j.ress.2022.108577.
35. Kendall MG. A new measure of rank correlation. Biometrika 1938; 30(1/2): 81–93. https://doi.org/10.2307/2332226.

Apendix A: Parameter estimation of the failure threshold distribution

The following maximum likelihood estimation method is provided to estimate $\boldsymbol{\theta}_D = (\mu_D, \sigma_D^2)'$.

Consider that there are k failed AC contactors of the same type. Let d_l for $l = 1,2,\cdots,k$ denote the cumulative arcing Joule integral of the failed

contact pair in the l-th AC contactor. Let d_{k+l} and d_{2k+l} for $l = 1,2,\cdots,k$ denote the respective cumulative arcing Joule integrals of the two functional contact pairs in the l-th AC contactor. Then, the likelihood function of $\boldsymbol{\theta}_D$ is written as

$$L_D(\boldsymbol{\theta}_D) = \prod_{l=1}^{k} \varphi\left(\frac{d_l-\mu_D}{\sigma_D}\right) \prod_{l=k+1}^{3k} \left(1 - \Phi\left(\frac{d_l-\mu_D}{\sigma_D}\right)\right) \quad \text{(A-1)}$$

where $\varphi(\cdot)$ and $\Phi(\cdot)$ are respectively the PDF and CDF of the standard normal distribution. Furthermore, the estimate of $\boldsymbol{\theta}_D$ is obtained by the genetic algorithm following the procedure as detailed in Subsection 4.1-1.

Apendix B: Algorithm for Generating the degradation data of an AC contactor

Algorithm 2: Generation of the degradation data for an AC contactor.

Input: The assumptions presented at the beginning of Appendix-B.

Output: The cumulative arcing Joule integrals $\{y_j(t), t = 0,1,2,\cdots\}$ for $j = A, B, C$.

Initialization: Let d_j, $x_j(t)$, and $y_j(t)$ be the realizations of D_j, $X_j(t)$, and $Y_j(t)$, respectively. Let $\Delta\tau_1$ and $\Delta\tau_2$ be the realizations of ΔT_1 and ΔT_2, respectively.

1: Set $\tau_b = 0$, $t = 0$, and $y_j(0) = 0$, and generate d_j from $N(4\,081\,942.3718,\ 6\,770.8431^2)$ for $j = A, B, C$.
2: **while** $y_j(t) < d_j$ for $j = A, B, C$ **do**
3: Set $t = t + 1$.
4: Generate $\Delta\tau_1$ and $\Delta\tau_2$ from $Exp(0.05)$ and $Exp(11.95)$, respectively.
5: Update $\tau_b = \tau_b + \Delta\tau_1 + \Delta\tau_2$. Then, compute $\phi_j(\tau_b)$ for $j = A, B, C$ according to (1).
6: Compute $x_j(t)$ for $j = A, B, C$ by substituting $\phi_j(\tau_b)$ into (6).
7: Compute $y_j(t)$ for $j = A, B, C$ using $y_j(t) = y_j(t-1) + x_j(t)$.
8: **end while**

Assume that the closing and breaking states of an AC contactor change over time following a two-state discrete-time Markov chain. Based on engineering experience, the durations of the closing and breaking states, denoted as ΔT_1 and ΔT_2, follow the exponential distributions with expected values of 0.05 and 11.95, referred to as $Exp(0.05)$ and $Exp(11.95)$, respectively. The current between the contact pair of phase j at instant τ_b is given by $i_j(\tau_b) = \sqrt{2}I\sin\left(\tilde{\phi}_j(\tau_b)\right)$, where $\tilde{\phi}_j(\tau_b) = \omega\tau_b + \theta_j$ with $\omega = 100\pi$ rad/s, $\theta_A = 0$ rad, $\theta_B = -2\pi/3$ rad, and $\theta_C = 2\pi/3$ rad. Additionally, I is set to 192 A, which is consistent with the AC-4 condition. Moreover, the following settings are formulated according to the parameter estimation based on the degradation data collected throughout the entire lifespans of Contactors #1 to #3 in Subsection 5.1. Assume that the failure thresholds $D_j, j = A, B, C$ of the three-phase contact pairs follow the normal distribution $N(4.0723 \times 10^6,\ 6.8766 \times 10^7)$. The two critical breaking phase angles of phase j are set as $\phi_j^L = 0.6152$ rad and $\phi_j^U = 3.0742$ rad for $j = A, B, C$.

Based on these assumptions, a Monte Carlo simulation algorithm, Algorithm 2, is proposed to generate the degradation data for an AC contactor.

Apendix C: Symbol explanation

Symbol	Description
	Arcing Mechanism analysis
$i_j(\tau)$	Instantaneous current of phase j at time τ
$\tilde{\phi}_j(\tau)$	Original phase angle of phase j at time τ
$\phi_j(\tau)$	Transformed phase angle of phase j at time τ
τ_b	Initial instant of a breaking process
ϕ_j^L, ϕ_j^U	Lower and upper critical breaking phase angles of phase j (parameters to be estimated)
$\tau_{j,arc}$	Arcing duration of phase j
x_j	Arcing Joule integral of phase j in an operation cycle
$L(\phi_j^U), U(\phi_j^L)$	Lower and upper bounds of arcing Joule integral for phase j
	Arcing mode evolution model
$M(t)$	Arcing mode in the t-th operation cycle ($M(t) = \text{I}, \text{II}, \text{III}, \text{IV}$)
$\boldsymbol{P}_t$	Transition probability matrix from operation cycle t to $t+1$
$P_{n,m}$	Transition probability from arcing mode n to mode m (parameters to be estimated)
$P_{\text{IV},m}(t)$	Transition probability from arcing mode IV to mode m in the t-th operation cycle
$W_n(t)$	Arcing mode similarity index between the imaginary mode n and the actual mode in the t-th operation cycle
$\boldsymbol{X}_{\text{I}}, \boldsymbol{X}_{\text{II}}, \boldsymbol{X}_{\text{III}}$	Random vectors of imaginary arcing Joule integrals in arcing modes I, II, and III
ε	Elastic factor in the arcing mode similarity index (a parameter to be estimated)
	Degradation Model

$Y_j(t)$	Cumulative arcing Joule integral of phase j up to the t-th operation cycle
$X_j(t)$	Arcing Joule integral of phase j in the t-th operation cycle
$x_j(t)$, $y_j(t)$	Observed values of $X_j(t)$ and $Y_j(t)$, respectively
$g_j(*)$, $G_j(*)$	PDF and CDF of arcing Joule integral for phase j when arcing occurs
$g_{k,l}(*,*)$	Joint PDF of arcing Joule integrals of phases k and l
$g_{A,B,C}(*,*,*)$	Joint PDF of arcing Joule integrals of phases A, B, and C
η_j, δ_j, ρ_j, λ_j, $\rho_{k,l}$, ν	Parameters to be estimated in $g_{k,l}(*,*)$
t_k	Current operation cycle number
$t_l^{n,m}$	Operation cycle marking the l-th transition from arcing mode n to mode m
$S_{j,1}$	Set of observed arcing Joule integrals of phase j prior to the current operation cycle
$S_{j,2}$	Observed arcing Joule integral of phase j at the current operation cycle
Failure Threshold	
D_j	Failure threshold of the contact pair of phase j
$\boldsymbol{\theta}_D = (\mu_D, \sigma_D^2)'$	Vector of parameters to be estimated in the failure threshold distribution